

**Universidade de Lisboa  
Faculdade de Ciências  
Departamento de Física**



**Control of Transcranial Brain Stimulation by a  
Brain-Computer Interface Based Loop**

Maria Inês Ferraz Meyer

**Dissertação**

Mestrado Integrado em Engenharia Biomédica e Biofísica  
Perfil em Sinais e Imagens Médicas

Novembro 2014



**Universidade de Lisboa  
Faculdade de Ciências  
Departamento de Física**



# **Control of Transcranial Brain Stimulation by a Brain-Computer Interface Based Loop**

Maria Inês Ferraz Meyer

## **Dissertação**

Mestrado Integrado em Engenharia Biomédica e Biofísica  
Perfil em Sinais e Imagens Médicas

**Orientador:**

Prof. Dr. Alexandre Andrade  
Instituto de Biofísica e Engenharia Biomédica  
Faculdade de Ciências  
Universidade de Lisboa

**Co-Orientador:**

Prof. Dr. Martin Bogdan  
Faculty for Mathematics and Computer Sciences  
Department of Computer Engineering  
University of Leipzig

Novembro 2014



# Contents

<b>Acknowledgements</b>	<b>V</b>
<b>Abstract</b>	<b>VII</b>
<b>Resumo</b>	<b>IX</b>
<b>List of Figures</b>	<b>XI</b>
<b>List of Tables</b>	<b>XIII</b>
<b>Abbreviations</b>	<b>XV</b>
<b>1 Introduction</b>	<b>1</b>
1.1 Motivation . . . . .	1
1.2 Thesis Layout . . . . .	2
<b>2 Fundamentals</b>	<b>5</b>
2.1 Electroencephalography (EEG) . . . . .	5
2.1.1 Background . . . . .	5
2.1.2 EEG Rhythms . . . . .	6
2.2 Brain Stimulation . . . . .	8
2.2.1 Background . . . . .	8
2.2.2 Transcranial Alternating Brain Stimulation (tACS) . . . . .	9
2.3 Brain-Computer Interfaces . . . . .	11
2.3.1 Background . . . . .	11
2.3.2 Mental strategies and brain signals in BCI . . . . .	12
2.3.3 General Purpose Platform for BCI Research - BCI2000 . . . . .	13

2.4	Methods for Analysis of EEG Signals . . . . .	14
2.4.1	Background . . . . .	14
2.4.2	Analysis of Statistical Properties of Signals . . . . .	14
2.4.3	Spectral Analysis . . . . .	14
2.4.4	Filtering Techniques and Artifacts . . . . .	15
2.4.4.1	Important Notes on Filters . . . . .	15
2.4.4.2	Artifacts . . . . .	16
2.4.5	Autoregressive Methods . . . . .	17
2.4.6	Methods for Phase Analysis . . . . .	18
2.4.6.1	Hilbert Transform . . . . .	18
2.4.7	Neural Synchrony . . . . .	20
2.4.7.1	Coherence . . . . .	20
2.4.7.2	Phase-Locking Value . . . . .	21
2.4.7.3	Phase Synchrony Index based on Entropy . . . . .	22
2.4.7.4	Verification of the Significance of Phase Synchrony - Surrogate Tests . . . . .	23
<b>3</b>	<b>Objectives</b>	<b>25</b>
3.1	Main Goals . . . . .	25
3.2	State of the Art . . . . .	26
3.3	Anticipated Problems . . . . .	27
3.3.1	Artifacts . . . . .	27
3.4	System Design . . . . .	29
<b>4</b>	<b>Methods</b>	<b>31</b>
4.1	Phase Evaluation . . . . .	31
4.1.1	PLV . . . . .	31
4.1.2	Analysis of Histogram - Entropy . . . . .	32
4.1.3	Peak-to-Peak Difference Analysis . . . . .	33
4.2	Algorithms for Closed-Loop Stimulation . . . . .	34
4.2.1	Processing of Analysed Signals . . . . .	34
4.2.2	Method 1: Phase Shift Approach . . . . .	36
4.2.3	Method 2: Adjustment Approach . . . . .	37

4.2.4	Method 3: Autoregressive Estimation of Reference . . . . .	38
4.3	Performance Evaluation of Algorithms . . . . .	39
4.3.1	Generation of Artificial Datasets . . . . .	39
4.3.2	Real Datasets . . . . .	39
4.3.2.1	Recorded Dataset . . . . .	39
4.3.2.2	Pre-recorded Datasets . . . . .	40
<b>5</b>	<b>Results</b>	<b>41</b>
5.1	Algorithms for Closed-Loop Stimulation . . . . .	41
5.1.1	Algorithms in Artificial Datasets - Proof of Concept . . . .	41
5.1.2	Selection of Size of Window and Step Interval . . . . .	42
5.1.3	Selection of best Method . . . . .	47
5.1.4	Application of selected Method to real data . . . . .	49
5.2	Analysis of Phase Stability . . . . .	50
5.2.1	Influence of Number of Contributing Oscillators on Simu- lated EEG Signals . . . . .	50
5.2.2	Comparison of Different Signal Types (Artificial and Real)	52
5.2.3	Comprehensive Analysis of Different Datasets . . . . .	53
5.2.3.1	cVEP Data . . . . .	53
5.2.3.2	ErrP Data . . . . .	55
5.2.3.3	Vigilance Data . . . . .	56
5.2.3.4	ECoG Data . . . . .	57
<b>6</b>	<b>Discussion and Conclusions</b>	<b>61</b>
6.1	Analysis and Discussion . . . . .	61
6.1.1	Algorithms for Closed-Loop Stimulation . . . . .	61
6.1.2	Analysis of Phase Stability . . . . .	62
6.2	General Conclusions and Future Directions . . . . .	64
	<b>Bibliography</b>	<b>67</b>





# Acknowledgements

First of all, I would like to thank Dr. Martin Spüler from the University of Tübingen, for his supervision, availability, and countless support. Without him this thesis would not have been possible.

A special acknowledgement is also in due to my supervisors Prof. Dr. Martin Bogdan, not only for his support, but also for accepting my internship in the wonderful city of Leipzig, and Prof. Dr. Alexandre Andrade, for all his advice and motivational words.

I would also like to thank Christopher Gundlach and Dr. Arno Villringer, from the Max-Planck Institute, for the opportunity to work together in this project.

I thank Filipa for helping me through the last five years, and making everything seem so much easier. Of course, I must also note the TI from the University of Leipzig. The people there showed me how much crazy is close to genius, and made last year unforgettable. A special thank you to Anke, for all the discussions, and helpful moments, and to Georg, for all the hints and tips, and hours of laughter.

Finally, I would like to dedicate this work to my family. In particular to my mother, Helena, without whom none of this would have been possible. Thank you for being the person I always look up to and admire the most.



# Abstract

Transcranial Alternating Current Stimulation (tACS) is a technique that enables the direct influence of ongoing brain oscillations. Among other after-effects, it has been shown to enhance perception to visual stimuli when started with the same phase as the ongoing brain oscillation of interest. Currently tACS is delivered using a feedforward paradigm, and thus it is very difficult to ensure that the parameters of stimulation meet the optimal requirements for studying a determined response. Thus, the present thesis proposes the use of Brain-Computer Interface (BCI) tools for devising a feedback loop to control the parameters of stimulation. Different methods are proposed and tested using artificial data. The best one is chosen, and tested on real Electroencephalogram (EEG) data. This yields surprisingly unstable results, that lead to a detailed investigation of the stability of the phase of real signals. Several datasets are analysed using systematic methodologies based on tools devised for the study of neuronal synchrony. The results for real signals are compared to artificially generated noise signals. It is shown that there is no evidence to support a claim of stability of phase behaviour along short time intervals, unlike what is assumed in classical EEG analysis. The present thesis presents an important step towards understanding a widely overlooked feature in EEG, and in tackling the problem of a feedback loop for tACS.



# Resumo

A Estimulação Transcraniana com Corrente Alternada (tACS) é uma forma de estimulação que permite a influência direta das oscilações cerebrais. Entre outros efeitos, foi demonstrado que quando a aplicação de tACS se inicia em fase com o sinal cerebral de interesse, a percepção a estímulos visuais apresentados aumenta. Presentemente, a aplicação de tACS não obedece a nenhum tipo de sistema de *feedback*. A estimulação é simplesmente iniciada num qualquer momento, o que dificulta o controlo sobre o tipo de efeitos em estudo. Como tal, a presente tese propõe a utilização de ferramentas do foro de *Brain-Computer Interfaces* (BCIs) na criação de um sistema fechado de controlo dos parâmetros da estimulação, nomeadamente a fase inicial. Assim, três metodologias para deteção dos parâmetros a partir do electroencefalograma (EEG) espontâneo e ajuste dos parâmetros de estimulação são propostos e testados em conjuntos de dados artificiais. O melhor dos três métodos é aplicado a um conjunto de dados de EEG real. O resultado é surpreendentemente instável (comparável ao obtido para um sinal de ruído Gaussiano). Assim, o foco da investigação muda para uma análise detalhada da estabilidade de sinais de EEG real, com base em metodologias inicialmente destinadas ao estudo de sincronia neuronal. Mostra-se que não há evidência para sustentar a assunção clássica de que a fase dos sinais cerebrais numa determinada banda de frequências é estável, pelo menos durante um curto intervalo de tempo. A presente tese representa um passo importante no sentido de compreender uma característica do EEG que muitas vezes se considera como bem conhecida e estudada, mas sobre a qual existem muitas dúvidas e lacunas de conhecimento. É ainda um avanço no problema de como aproximar um sistema de controlo fechado para tACS.



# List of Figures

2.1	Conduction of a nerve signal in an unmyelinated fibre. . . . .	6
2.2	Electrode placement in 10-20 system. . . . .	7
2.3	Model prediction of how a network of neurons would behave in response to AC stimulation. . . . .	10
2.4	Possible effects of weak AC stimulation. . . . .	11
2.5	BCI2000 design. . . . .	13
2.6	Comparison of a power spectrum over the whole signal and the periodogram calculated with Welch method. . . . .	16
2.7	Representation of the Hilbert Transform. . . . .	19
3.1	EEG recorded during tACS session. . . . .	28
3.2	Basic design of the closed loop tACS/BCI system. . . . .	30
4.1	Illustration of the phase series resulting from the application of the Hilbert Transform. . . . .	32
4.2	Example of distribution of phase difference. . . . .	33
4.3	Application of Welch method for estimation of power spectrum. .	35
4.4	Representation of one segment and the defined intervals for appli- cation of the algorithms. . . . .	36
4.5	Illustration of the basic procedure used in the adjustment approach.	37
4.6	Method 3: Predicted time series against the original pre-processed simulated EEG signal. . . . .	38
5.1	Methods for generation of stimulation signal: proof of concept. . .	43
5.2	Comparison of PLV and phase difference over analysed windows for different window and step interval sizes. . . . .	46

5.3	Comparison of the outcome of the three methods. . . . .	48
5.4	Phase Adjustment Method applied to real signals. . . . .	49
5.5	Average peak-to-peak distance and PLV according to number of contributing oscillators of simulated EEG signals. . . . .	51
5.6	Comparison of the average values of mean, peak-to-peak difference, PLV and synchrony index for each signal contained in the dataset.	52
5.7	PLV and synchrony index for cVEP data. . . . .	54
5.8	Peak-to-peak difference and PLV for ErrP data. . . . .	55
5.9	Peak-to-peak difference and PLV for Vigilance data. . . . .	57
5.10	Peak-to-peak difference and PLV for ECoG data. . . . .	58



# List of Tables

5.1	Average values for application of the methods to sine waves and Gaussian noise. . . . .	42
5.2	Phase difference for different window and step andvance combinations.	44
5.3	PLV for different window and step andvance combinations. . . . .	45
5.4	Average values for each method over the same simulated EEG dataset.	47
5.5	Comparison of the average values for real, noisy and simulated EEG signals. . . . .	50
5.6	Average results of stability tests for cVEP data. . . . .	54
5.7	Average results of stability tests for ErrP data. . . . .	56
5.8	Average results of stability tests for Vigilance data. . . . .	57
5.9	Average results of stability tests for ECoGdata. . . . .	58



# Abbreviations

<b>BCI</b>	Brain-Computer Interfaces
<b>CAR</b>	Common Average Reference
<b>ECoG</b>	Electrocorticogram
<b>EEG</b>	Electroencephalogram
<b>ERP</b>	Event Related Potentials
<b>ERS/D</b>	Event Related Synchronization/Desynchronization
<b>FFT</b>	Fast Fourier Transform
<b>fMRI</b>	functional Magnetic Resonance Imaging
<b>FT</b>	Fourier Transform
<b>HT</b>	Hilbert Transform
<b>PLS</b>	Phase-Locking Statistics
<b>PLV</b>	Phase-Locking Value
<b>SCP</b>	Slow Cortical Potentials
<b>SMR</b>	Sensorimotor Rhythms
<b>SSVEP</b>	Steady-State Visually-Evoked Potentials
<b>tACS</b>	transcranial Alternating Current Stimulation
<b>PS</b>	Power Spectrum



# 1 Introduction

The present thesis is the result of a one year cooperation between the Faculty of Sciences of the University of Lisbon with the University of Leipzig, Department of Mathematics and Computer Sciences, and the Max Planck Institute for Human Cognitive and Brain Sciences, Department of Neurology. The project included a collaboration with the University of Tübingen, through the BCI Project group.

This chapter introduces the general theme and motivation for the project, and outlines the following chapters.

## 1.1 Motivation

Transcranial Alternating Current Stimulation (tACS) consists of the external application of oscillating electrical currents to the brain. This technique makes it possible to influence the cortical excitability and activity through direct modulation of the ongoing brain oscillations. These are associated with brain functions, as has been shown in several studies over the past years [1, 2, 3]. Parameters such as the amplitude of a brain rhythm and its phase at the moment of presentation of a stimulus are shown to have an influence on the perception of this stimulus [4, 5]. Thus, the possibility to alter these oscillations is of great interest for a better understanding of the underlying brain processes and for a possible application to patients with neuropsychiatric disorders characterized by aberrant oscillatory activity (e.g., schizophrenia).

There is particular interest in controlling the onset of the stimulation. It has been shown that the perception of visual stimuli is increased when tACS is delivered in phase with the ongoing brain rhythm of interest [2]. Currently, tACS stimulation is based on a feedforward paradigm where the moment when to start is not taken into account. The referred observation is done by offline analysis of the electroencephalogram (EEG) at the moment immediately before stimulation. Thus, a big improvement could be achieved if

the onset of stimulation could be controlled. This would require an online analysis of the ongoing oscillatory activity, and a pre-adjustment of the stimulation signal to be delivered.

The present thesis proposes an approach to this particular problem using Brain-Computer Interface (BCI) based tools. Online, real time processing is done every day in BCI use, and thus, to link the already existing solutions to tACS stimulation seems nothing but logical. It is here proposed that a feedback loop based on BCI is used to control the onset of stimulation in phase with the ongoing brain signals. Such a control system could be used to adjust other parameters, hence providing a new tool for research, and potentially improving the use of tACS in a real life therapeutic application.

The present thesis starts by developing and comparing three different approaches to the problem of detecting the parameters of interest from the spontaneous EEG, and adjusting a stimulation signal to be started in the correct moment, regarding phase. As the project progresses, the path of research is forced to change, since the methodologies reveal a very high degree of instability in the phase of the ongoing brain oscillations. Hence, the stability in terms of phase of the ongoing signal becomes the main focus point, since the type of system that is proposed is not possible unless the EEG presents a certain degree of temporal stability.

The main conclusion is that, unlike what is assumed in classical analysis of EEG, the phase of the ongoing signals has very unstable dynamics. This is connected to the fact that the oscillations are the result of the dynamics of thousands of different neurons oscillating simultaneously. Due to this fact, the suggested approach does not work with real signals, and it is unclear if an *in-phase* stimulation is at all possible with an unstable phase.

## 1.2 Thesis Layout

The present thesis is divided into six chapters (including the ongoing one). The chapter to follow covers the fundamental background necessary for understanding the approaches, methodologies and the motivation of the project. This includes a deeper look at the basics of EEG, an introduction to tACS and BCI, and finally the most important signal processing techniques used in the present work. A chapter devoted to outlining the main goals, expected problems, and design of the proposed system

follows. This brief chapter locates the project with other research, and clearly states the problem to be dealt with, as well as the approach to be used. As a logical step, Chapter 4 presents the most relevant methodologies applied in the course of the project. The results produced by their implementation are described in Chapter 5. At this point, a very important result regarding the phase of the ongoing signals forces a change of the main focus of the project. Thus, the second part of Chapter 5 deals with the problem of phase stability over time. A detailed analysis is performed to several sets of real data, using a systematic approach. Finally, some conclusions regarding the results are taken and discussed in Chapter 6. A general evaluation is also done here, and possible future approaches to deal with both the original loop problem and the encountered phase stability are proposed.





## 2 Fundamentals

In the current chapter an overview of the most important background concepts for understanding the motivation, methods and conclusions is given. A brief introduction to EEG, making note of the most important basics, is followed by a section addressing transcranial Alternating Current Stimulation. Brain-Computer Interfaces are also introduced. The last section provides a description of concepts and techniques regarding signal processing that are of importance in the context of the thesis. í

### 2.1 Electroencephalography (EEG)

#### 2.1.1 Background

Signals within the brain propagate in the form of electric impulses. These impulses are manifested by the generation of action potentials and postsynaptic potentials, which result in the transmission of the signal from neuron to neuron. Neurons are formed by a body, or soma, surrounded by dendrites, an axon and synaptic terminals. Most incoming signals enter the neuron through synapses located in the dendrites. From here they travel through the single axon that leaves the body of the neuron, due to the generation of action potentials. Such potentials are connected with changes in the ionic permeability of the axonal membrane that cause a fast increase and decrease of the membrane voltage, and thus a change in the polarity of the intracellular medium. Once it begins, the action potential travels peripherally along the axon until it reaches the terminal arborization. Once at the synaptic terminals it triggers the release of neurotransmitters that stimulate the next cell across the synapse [6]. The neurotransmitters will produce postsynaptic potentials that can result in excitation of the next neuron or its inhibition. The basic propagation principle is illustrated in Figure 2.1.

The described electrical activity generates currents along the cell membrane in the intra- and extracellular spaces and produces an electric field that approximates that of a

## 2. Fundamentals

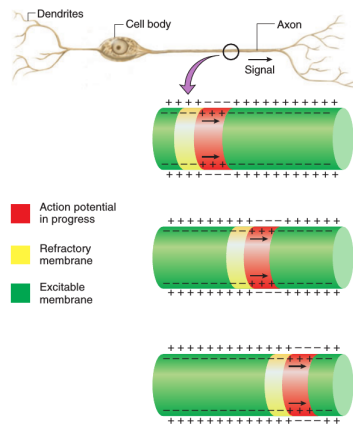


**Figure 2.1:** Conduction of a nerve signal in an unmyelinated fibre. The membrane polarity is reversed in the region where the action potential takes place (red). The region depicted in yellow is the refractory period - it can not be excited and thus prevents the signal from travelling backwards. Retrieved from [6].

dipole [7]. The synchronous action of these neurons translates into an overall electrical activity that, if the number of neurons is large enough, can be macroscopically observed.

The first and still one of the most used methods for detecting this activity is the Electroencephalogram (EEG). It consists of the recording of the macroscopic cooperative action of the brain cells and can be acquired through electrodes placed on the scalp or directly on the cortex (in which case it is referred to as Electrocorticogram (ECoG)). In the case of scalp electrodes, they can be secured by an adhesive or embedded in a special cap [7]. The displacement of the electrodes is standardized to facilitate data interpretation and comparison. One of the most common displacement systems is the international 10-20 system depicted in Figure 2.2.

### 2.1.2 EEG Rhythms

The brain waves recorded by EEG are rhythmic voltage changes that, as mentioned before, stem from synchronized postsynaptic potentials in the superficial layers of the cerebral cortex [6]. Alterations in these brain waves are related to age, behavioural state of the subject, neuro-pathological conditions, degenerative brain diseases, or drug action, among other influencing factors. Several rhythms were identified in EEG, distinguished by differences in amplitude (mV) and frequency (Hz). The delta ( $\delta$ ) rhythm ranges from 0.5 to 4 Hz and has high amplitudes; it is predominant during sleep for adults and is

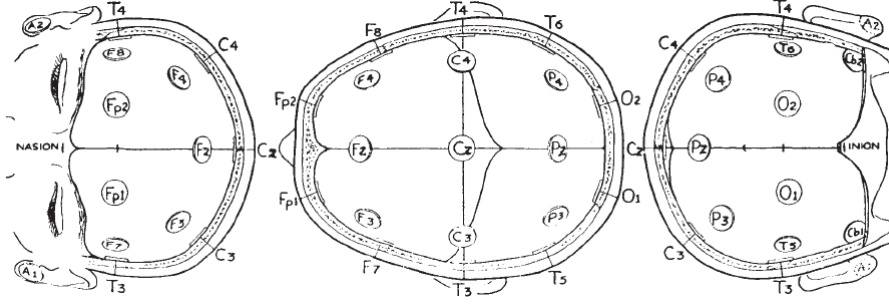


**Figure 2.2:** Electrode placement in 10-20 system. 19 electrodes are placed related to specific anatomic landmarks, such that 10-20 % of the distance between them is used as the electrode interval. Retrieved from [7].

present in infants during the awake state. Waves in the next frequency band, from 4 to 8 Hz, are classified as theta ( $\theta$ ) rhythm; these are present in certain emotional or cognitive states and may be connected with pathology [7]. The most widely studied rhythms are in the 8 Hz to 13 Hz band - alpha ( $\alpha$ ) and mu ( $\mu$ ) waves; the  $\alpha$  rhythm is predominant during an awake and relaxed state (at best with closed eyes), being best observed in the posterior regions of the head. It is attenuated by focused attention and mental effort. As for the  $\mu$  rhythm, it is related to the function of the motor cortex and is thus predominant in the central part of the head; these waves are attenuated by movement. In the bandwidth from 13 to 30 Hz the beta ( $\beta$ ) rhythm occurs; it is observed in the frontal to parietal region and is characteristic of focused attention, increased alertness and sensory stimulation. Finally, frequencies above 30 Hz are connected to gamma ( $\gamma$ ) activity; this rhythm is present during information processing and voluntary movement. In a very general way, it can be summarized that the slowest cortical rhythms are related to a resting brain, while the fast rhythms are an indicator of information processing [7].

The oscillations in EEG are not only characterized by their power, but also by their instantaneous phase. The oscillatory phase of the signal at a given frequency reflects cyclic fluctuations of a network's excitability. These fluctuations occur on much shorter time scales than variations in oscillatory power at the same frequency [4, 8]. However, the physiological background of this oscillatory behaviour is poorly understood, and so is the influence of the oscillatory phase in processes such as perception. Several studies have tried to understand the underlying mechanisms and investigated the EEG processes by analysing the spontaneous signals [9, 10], or responses to stimuli, i.e., evoked potentials [11, 4]. It has been demonstrated that a relationship exists between the phase of the spontaneous EEG and the amplitude of subsequent Event Related

Potentials [5]. More recently, the hypothesis that the phase of ongoing oscillations may represent an indicator of perceptual cycles, such that a stimulus appearing at the optimal phase would be optimally registered and perceived, was tested [4]. This hypothesis was validated, and thus it is recognized that the perception of a visual stimulus is enhanced or attenuated depending on the phase of spontaneous EEG at the time of presentation of the stimulus. Such fact puts a focus on the phase of the ongoing EEG as an important parameter to be taken into account during presentation of stimuli. Specifically, the mentioned effect was studied in connection with transcranial brain stimulation, and seen to also produce a change in perception [12, 13].

## 2.2 Brain Stimulation

### 2.2.1 Background

The brain is known to adjust and adapt. The existing neuronal connections undergo dynamic changes that may be followed by the establishment of new connections in the cortex [14]. This can be due to an accident, the learning of a new task or a behavioural response. It is currently accepted that with the acquisition of new skills the brain changes through a rapid reinforcement of pre-established organic pathways and later formation of new pathways. The nervous system is thus a continuously changing structure of which plasticity is an integral property and a consequence of each sensory input, motor action, reward signal, action plan, awareness or mental association [14].

The possibility of influencing this process has been a topic of interest in research for several decades. External influences on neuroplastic processes may be used for functional improvement of diseases and in particular for improving cortical functions such as learning [15]. As the processes in the brain are mostly governed by electrical discharges, it has been hypothesized that the application of weak electrical fields in active neuronal networks can induce slight changes in the firing rate of neuronal populations [16, 12].

One of the most successful and known methods at present is Transcranial Magnetic Stimulation (TMS). This technique is based on the principle of electromagnetic induction of an electric field in the brain [17]. If the magnetic field has a sufficiently high magnitude and density it can depolarize neurons. In a different approach, if the magnetic pulses are applied in a repetitive way it becomes possible to increase or decrease cortical

excitability. Other techniques exist that result in such neuroplastic-like effects. One of such is transcranial Direct Current Stimulation (tDCS). In this case a weak direct current is passed through the skull, thus applying an electric field that makes it easier (or harder, depending on the polarity) for neurons to reach the excitatory threshold, and thereby increasing or decreasing their firing rate. The after effects are comparable to the ones observed in repetitive TMS (rTMS), but tDCS avoids the risk of potentially inducing seizures [15]. Stimulation can also be performed with a random noise frequency spectrum, which is called transcranial Random Noise Stimulation (tRNS). The application of such signals produces a stochastic resonance-like effect, making it easier for neurons to reach the threshold. The neuroplastic effects of tRNS are once again similar to the effects obtained with tDCS, but here only excitatory after effects are observed.

### 2.2.2 Transcranial Alternating Brain Stimulation (tACS)

The type of transcranial stimulation of interest in the scope of the present work applies alternating currents to the scalp. In transcranial Alternating Current Stimulation (tACS) the current alternates between the anode and the cathode, usually with a sinusoidal waveform (although any other type of waveform is possible) [16]. The predominant hypothesis is that alternating fields can increase or decrease power of oscillating rhythms in the brain in a frequency-dependent manner by synchronizing or desynchronizing neuronal networks [18]. Since then it has been shown that the transcranial application of sinusoidal alternating current is able to modify the discharge of spontaneously active neurons and cortical oscillations in humans, and that it achieves this effect in a painless, selective, non-invasive and reversible way [19, 20]. It thus has the potential to modulate physiologically relevant brain oscillations in a frequency-specific manner [1], and affect cognitive performance. As such it may potentially be used in the treatment of neurological disorders [18].

At a cellular level, Alternating Current (AC) fields will alter the transmembrane potential of pyramidal cells sinusoidally and proportionally to the field intensity. The efficacy of AC field frequency derives from the passive properties of biological membranes (which act like a low-pass filter). Although the effects of AC stimulation on a single neuron are expected to be smaller than the effects of the application of DC fields, networks of neurons can exhibit higher sensitivity to AC fields [18].

It was demonstrated in [13] by the use of a simplified Hodgkin-Huxley model that the firing rates of inhibitory and excitatory neurons are up- and down-regulated in phase

## 2. Fundamentals

---

with the AC current without changing the average firing rate over a longer time interval. At the same time, it was shown that when this stimulation is at the same frequency as ongoing oscillations of interest, it mainly affects the timing of spikes. Even at low amplitudes, stimulation results in enhanced coherence between spikes and the driving oscillation [1]. Figure 2.3 illustrates this effect. It is currently accepted that the phase

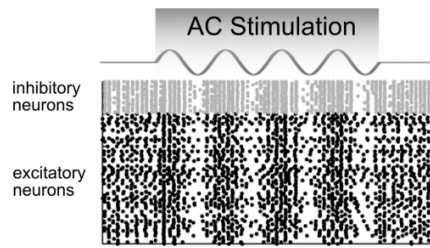


**Figure 2.3:** Model prediction of how a network of neurons would behave in response to AC stimulation. The firing rates are up- and down-regulated in phase with the AC current. Inhibitory neurons are represented in grey and excitatory neurons in black. Each dot represents a neural spike. Retrieved from [1].

of  $\theta$  oscillations modulates the amplitude of gamma oscillations. Hence, were the cortex to be stimulated at frequencies in the  $\theta$  range, the phase of these artificial  $\theta$  oscillations could modulate the amplitude of  $\gamma$  oscillations [1]. Such effect could be achieved by the neural mechanism demonstrated in [13] and illustrated in Figure 2.3. Some findings further indicate that tACS is capable of modulating ongoing somatosensory oscillations (in this case,  $\mu$ -rhythm) only when the exact individual frequency of the respective rhythm is applied [3].

AC stimulation can entrain the oscillations by shifting their phase or modulating their power at the stimulation frequency. This effect is illustrated in Figure 2.4. It was in [2] that tACS applied at the individual alpha frequency of the participants resulted in an enhancement of the EEG amplitude after 10 minutes of stimulation. The spectral power of the signal was significantly increased in the range of the individual alpha frequency, when compared to the signal before stimulation onset. This indicates that the method can interfere with ongoing brain oscillations in a frequency-specific way, despite its low amplitude and its transcranial application.

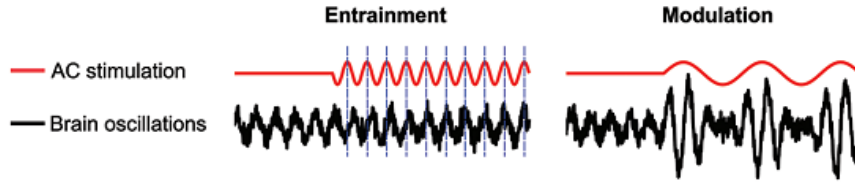


**Figure 2.4:** Possible effects of weak AC stimulation. Signals can be entrained by a shift in their phase (left) , or modulated at the stimulation frequency (right). Retrieved from [18].

## 2.3 Brain-Computer Interfaces

### 2.3.1 Background

Brain-Computer Interfaces (BCIs) are a particular case of Human-Machine Interaction (HMI). They measure brain activity, process it, and produce control signals that reflect the user's intent [21].

The main goal of BCI research is to provide new communication and motor pathways for severely impaired patients (while providing a powerful working tool in computational neuroscience [22]). Signals are detected directly from the brain and transmitted to a processing station. Hence, BCIs provide communication and control channels that do not depend on the brain's normal output channels, composed by peripheral nerves and muscles [23].

The interaction of the user with the device to be controlled is enabled by intermediary functional components, control signals and feedback loops [24]. The system itself consists of a closed loop of which the user and the device are integral parts. Feedback loops inform each component in the system of the state of one or more of the other components [24]. The neuronal activity is sampled in real time and translated into commands that are used to control a given application [22], such as a communication device [25].

Brain activity can be measured by non-invasive techniques (e.g., EEG, functional Magnetic Resonance Imaging (fMRI)) or by invasive ones (e.g., Electrocorticogram (ECoG), intracortical recordings). The most widely used recording technique in BCI is EEG, due to factors such as its good temporal resolution, relatively low cost, high portability, safety and few counter indications. When using EEG signals, several types of features can be used, depending on the paradigm of the BCI itself. Specific features of the EEG can be regulated by the user (e.g., Slow Cortical Potentials (SCPs), Sensorimotor

Rhythm (SMR)) or be elicited by sensory stimulation (Event Related Potentials (ERPs) - P300 or Steady-State Visually-Evoked Potentials (SSVEP)) [22].

### 2.3.2 Mental strategies and brain signals in BCI

A BCI can only detect and classify patterns of activity in the ongoing brain signals that are associated with specific tasks or events. As such, the mental strategy is the foundation of any Brain-Computer interaction: It determines what the user has to do in order to produce brain patterns that the BCI can interpret. The mental strategy influences the type of analysis and yields information that is useful for different types of application. The most common mental strategies are selective attention and motor imagery [21]. Selective (focused) attention requires external stimuli, such as flashing symbols in a screen. The user will focus his/her attention on the symbols of interest, each of which will correspond to a command. Focusing the attention on the desired symbol will elicit a response in the EEG when it flashes. Motor imagery consists in the imagination of movement, which produces changes in the Sensorimotor Rhythm (SMR).

Different types of mental strategy elicit patterns in the EEG. It is possible to analyse these patterns using different methods. Thus, two main groups of BCI can be considered:

**Analysis in the time domain** The most widely used feature is the so called P300, which is a positive deflection of the EEG that occurs approximately 300 ms after the presentation of a certain kind of stimulus. Another type of pattern, the so called Error Related Potentials (ErrPs) are elicited when the user perceives a mistake.

**Analysis in the frequency spectrum** Steady-State Visually Evoked Potentials (SSVEPs), resulting from selective attention, will appear on the EEG as a power increase at the same frequency as the presented flickering stimulus. Thus, a SSVEP BCI can determine which stimulus occupies the user's attention by looking for SSVEP activity in the visual cortex at a specific frequency. Changes in the SMR due to motor imagery are also analysed in the frequency spectrum. A decrease of oscillatory activity in a specific frequency band is an Event Related Desynchronization (ERD), while an increase of the same activity is an Event Related Synchronization (ERS). Movement or preparation for movement is usually accompanied by an ERD; after the movement and with relaxation an ERS occurs. The most important frequency bands for motor imagery are  $\mu$  (8 - 12 Hz) and *beta* (12 - 30 Hz).



### 2.3.3 General Purpose Platform for BCI Research - BCI2000

The authors of [26], developed a general-purpose BCI platform - the BCI2000. This arose from the need to evaluate and compare different methods and new applications in a systematic way. Before that, most BCI systems were designed specifically for one particular method of interest and therefore could not be generalized and compared to other systems. Another known weakness of BCI research was the difficulty to incorporate and compare diverse brain signals, processing methods and output modalities.

The BCI2000 platform is based on a model and on general principles that can describe most BCI systems. It consists of four modules (refer to Figure 2.5). Each module is as independent from the others as possible, and encompasses the related BCI functions - source (data acquisition and storage), signal processing, user application and operator interface. These modules and the communication protocol between them do not place constraints on the major parameters for BCI architecture (i.e., number of signal channels, sampling rate, system parameters, event markers, complexity of signal processing, timing of operation and number of signals that control the output device) [26]. Data gathered during online operation can be stored for offline analysis. Another advantage of BCI2000 is that it offers a set of ready-to-use methods for researchers interested in applying known methods to groups of subjects. It is still possible to build on the existing modules, to improve or adjust them to the current need.

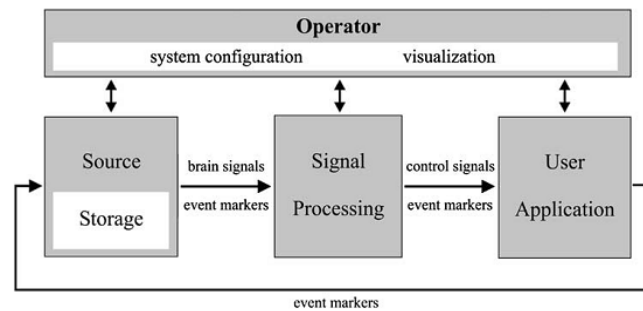


**Figure 2.5:** BCI2000 design. Comprises four modules: operator, source, signal processing and application. Retrieved from [26].

## 2.4 Methods for Analysis of EEG Signals

### 2.4.1 Background

The EEG time series can be seen as a realization of a stochastic process. Its statistical properties can thus be evaluated by typical methods based on the theory of such signals. These include probability distributions and their moments (i.e., mean and variances), correlation functions and spectra. For the sake of simplicity these properties are assumed not to change during the observation time. However, this is not necessarily true, as EEG signals are non-stationary. Still, they can be subdivided into quasi-stationary epochs when recorded under constant behavioural conditions, which allows the assumption of stationarity when estimating the aforementioned properties [7]. The analysis of this type of signal can be done in the time or frequency domain. In order to deal with the non-stationarity, time-specific methods are often used. Methods that aim at removing the non-stationary parts of the signal using linear methods [27] have been attempted. Some authors used non-linear methods for the analysis. Most are based on estimators derived from chaos theory, such as attractor dimension or Lyapunov coefficients. However, these parameters do not provide a significant improvement in the analysis, as the EEG shows a coloured noise-like behaviour and a chaotic character only in some epochs, usually related to the occurrence of epileptic seizures. Moreover, the above mentioned chaotic estimators require long stationary data epochs, are subject to systematic errors and are very sensitive to noise [7].

In the following subsections some important background concepts for the present text are described. The first topics covered are signal processing generalities, such as the power spectrum, filtering techniques, windowing and autoregressive models. Followed by this is a number of methods and concepts important for understanding and analysing the phase of signals. The Hilbert Transform and methods for estimating neural synchrony are described.

### 2.4.2 Analysis of Statistical Properties of Signals

### 2.4.3 Spectral Analysis

The Power Spectrum (PS) of a signal answers the question "How much of the signal power is at frequency  $\omega$ ?" [28]. In other words, it provides the distribution of a signal's power (energy per unit time) over determined frequency bins.

Following the definition in [29], the power spectrum is commonly described as the Fourier transform of the autocorrelation function:

$$PS(f) = \sum_{n=0}^{N-1} r_{xx}(n) e^{-j2\pi n f T_s} \quad (2.1)$$

It can be calculated using a more direct approach, which is motivated by the fact that the energy contained in an analogue signal  $x(t)$  is related to the square of the signal integrated over time:

$$E = \int_{-\infty}^{\infty} |x(t)|^2 dt \quad (2.2)$$

When transposed to the frequency domain through a Fourier Transform, it is possible to infer that  $|X(f)|^2$  equals the energy density function over frequency - the power spectrum:

$$PS(f) = |X(f)|^2 \quad (2.3)$$

When the available time series is only a sample of a longer signal, the PS becomes an estimation process. In such cases, averaging the PS improves its statistical properties. This process produces what is commonly referred to as an average periodogram. One of the most widespread methods for computing the periodogram is the Welch method. Here the data is divided into several segments, which may overlap; the Fast Fourier Transform (FFT) is calculated for each of the segments, from which the PS is calculated, and these spectra are finally averaged. The power spectrum and the periodogram of a signal are represented in Figure 2.6.

## 2.4.4 Filtering Techniques and Artifacts

### 2.4.4.1 Important Notes on Filters

The goal of filtering is to reshape the spectrum to one's advantage. This spectral reshaping can be achieved by two different types of approach: *finite impulse response* (FIR) filters or *infinite impulse response* (IIR) filters. FIR filters have transfer functions that have only numerator coefficients, which leads to a finite impulse response. Thus, they are always stable and have linear phase shifts, but are non-recursive. An IIR filter, on the other hand, has a transfer function composed by a numerator and denominator.

## 2. Fundamentals

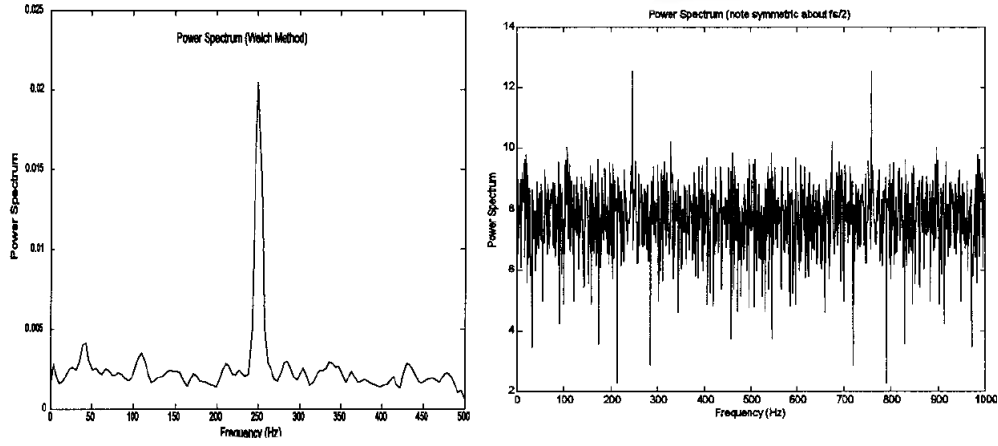


**Figure 2.6:** On the right is the periodogram calculated using the Welch method. On the left, the power spectrum over the entire signal. Both derive from the same signal. When applying the Welch method there is an improvement in the background spectra, but the peak at 250Hz becomes broader. Note that the Power Spectrum is symmetric over the sampling frequency, and the periodogram is represented only from 0 Hz to the sampling frequency (500Hz). Adapted from [29].

The main advantage is that these filters can meet specific frequency criteria (i.e., cutoff sharpness, slope) with lower filter order. Many of the concepts of analog filters can be used in the design of a digital IIR filter. Namely, well known filter types can be implemented, such as Butterworth, Chebyshev and elliptic filters. Butterworth filters have a flat frequency response in the passband, thereby compromising rolloff steepness [29].

**Zero-phase (Even Impulse Response) filter** A zero-phase filter avoids any distortions in the phase of the signal, since its phase slope is  $\alpha = 0$ . It satisfies the condition:  $h(n) = h(-n)$ ,  $n \in \mathbb{Z}$

It is characterized by an impulse response that is symmetric around sample zero. When the Fourier Transform of the waveform is taken, the phase is zero. It is possible to modify recursive filters by using a bidirectional technique. When combining forward and backward filtering a zero-phase recursive filter is produced.

### 2.4.4.2 Artifacts

Artifacts are errors in the signals introduced by equipment, processing techniques, or environmental factors. In the particular case of EEG, eye movement will create

deflections in frontal electrodes, and jaw movements will produce deflections across the electrode readings; external factors may cause disruptions that are common to all electrodes. There are several techniques to minimize the effect of artifacts. In the case of eye movement, the usual procedure is to measure the electrooculogram (EOG) and subtract it from the affected signals. Another commonly used procedure is Common Average Referencing.

**Common Average Referencing (CAR)** This technique has the purpose of reducing noise that is common to all electrodes. It adjusts the signal at each electrode by subtracting the average of all electrodes.

$$y_i = x_i - \frac{1}{N}(x_1 + \dots + x_N), \quad i = 1, 2, \dots, N \quad (2.4)$$

However, this method does not reduce noise that is not present in all the electrodes [21].

Other techniques for artifact removal exist that target more specific cases, or regions. These methods are, however, not in the scope of the present thesis.

### 2.4.5 Autoregressive Methods

Autoregressive methods are a form of statistical modelling of a stochastic process. The main goal is to produce a mathematical model that represents the system that generates the process. The term autoregression refers to the use of the previous values of the output  $X_{t-k}$  to estimate the current output  $X_t$ .  $X_t$  is a linear combination of the past outputs and a white noise input ( $\epsilon_t$ ). Thus, an autoregressive model of order  $p$ , AR( $p$ ), is defined in the time domain as:

$$y[n] = c + \sum_{k=1}^p \alpha_k X_{t-k} + \epsilon_t \quad (2.5)$$

where  $c$  is a constant and  $\alpha_k$ ,  $k = 1, 2, \dots, p$ , are the coefficients of the model of order  $p$ .

There are several types of approaches for estimating the coefficients of the model directly from the waveform. The most widely used are the Yule-Walker, the Burg, the covariance and the modified covariance methods. The most appropriate method will depend on the expected shape of the spectrum. The Yule-Walker method is thought to

produce the spectra with the least resolution among the four, but provides the most smoothing [29].

A low order AR model smooths the noise very effectively. Higher order models result in better frequency resolution, but the noise is not effectively reduced.

The best order of a model can be chosen using Information Criteria, namely Akaike's Information Criterion (AIC) or Bayesian Information Criterion (BIC). These are likelihood based measures of the fit of a model that include a penalty for complexity (number of parameters of the model). The best order is the one that minimizes the value of AIC or BIC.

### 2.4.6 Methods for Phase Analysis

#### 2.4.6.1 Hilbert Transform

The Hilbert Transform (HT) of a function  $g(t)$  can be considered as the convolution of this function with  $1/\pi t$ , where  $t$  represents time. This means that the HT can be realised by an ideal filter whose amplitude response is unity and phase response a  $\pi/2$  lag at all frequencies [30]. It is formally defined as [31]:

$$H[g(t)] = g(t) * \frac{1}{\pi t} = \frac{1}{\pi} \int_{-\infty}^{\infty} \frac{g(\tau)}{t - \tau} d\tau = \frac{1}{\pi} \int_{-\infty}^{\infty} \frac{g(t - \tau)}{\tau} d\tau \quad (2.6)$$

After dealing with the improper integral (i.e., the integrand has a singularity and the limits of integration are infinite) in the definition of the HT, the new definition of the transform is [31]:

$$H[g(t)] = \frac{1}{\pi} \lim_{\epsilon \rightarrow 0^+} \left( \int_{t-1/\epsilon}^{t-\epsilon} \frac{g(\tau)}{t - \tau} d\tau + \int_{t+\epsilon}^{t+1/\epsilon} \frac{g(\tau)}{t - \tau} d\tau \right) \quad (2.7)$$

The Hilbert Transform is useful in calculating instantaneous attributes of a time series. Instantaneous amplitude and phase are basic concepts in all the questions dealing with modulation of signals appearing especially in communication or information processing.

The analytic signal  $z(t)$  of a real-valued signal  $s(t)$  is defined as [32]:

$$z(t) = s(t) + jH[s(t)] \quad (2.8)$$

where:  $s(t)$  is the input signal and  $H[s(t)]$  is the Hilbert Transform of the input signal.

The real and imaginary parts can be expressed in polar coordinates as:

$$z(t) = A(t)\exp[j\psi(t)] \quad (2.9)$$

where  $A(t)$  is the envelope or amplitude of the analytic signal, and  $\psi$  is the phase of the analytic signal. The derivative of  $\psi$  returns the instantaneous frequency of the signal.

Thus, the instantaneous amplitude is the amplitude of the complex Hilbert Transform; the instantaneous frequency is the time rate of change of the instantaneous phase angle. For a pure sinusoid, the instantaneous amplitude and frequency are constant. Figure 2.7 represents the real and imaginary parts of the HT, as well as the instantaneous amplitude and phase that can be retrieved from it.

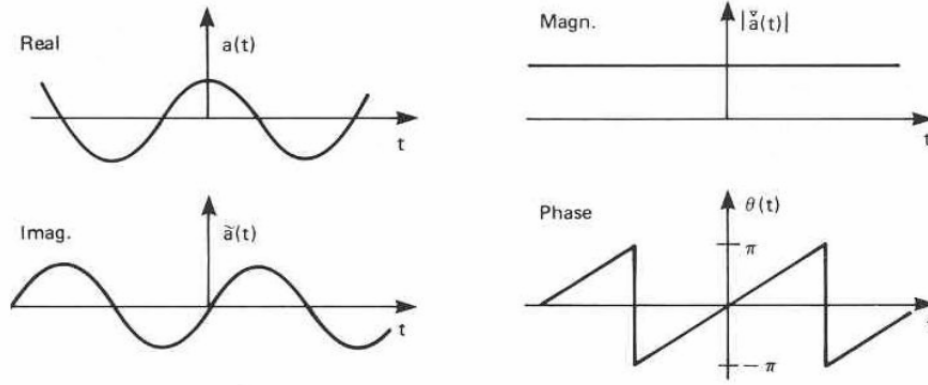


**Figure 2.7:** Real and imaginary parts of the Hilbert Transform, and the representation of instantaneous phase and magnitude of the signal over time. Note that the phase is shifted  $\pi/2$  radians relatively to the original signal. Adapted from [33].

The analytic signal  $z(t)$  of a time series has a one-sided Fourier Transform (FT). That is, the transform vanishes for negative frequencies. Considering  $Z(\omega)$  as the FT of  $z(t)$  and  $S(\omega)$  the FT of  $s(t)$ :

$$Z(\omega) = \begin{cases} 2S(\omega) & \omega > 0 \\ S(\omega) & \omega = 0 \\ 0 & \omega < 0 \end{cases}$$

In the frequency domain the algorithm used by the HT consists in taking the Discrete Fourier Transform (DFT) of the discrete signal (here termed  $s(n)$ ), setting its negative

frequency bins to zero but doubling its positive frequency bins and obtaining the discrete analytic signal  $z(n)$  by the inverse FT of the spectra.

In this definition of instantaneous phase, the signal  $s(t)$  must be narrow-band in the frequency domain [32], and thus a broader band signal should be filtered around a narrower frequency band for analysis. To derive the analytic signal, it is necessary to shift the phase of the original signal by 90 degrees, due to the definition of the HT.

The HT does not change domains. A time domain function remains in the time domain, and a frequency domain function in the frequency domain. The result is similar to an integration.

### 2.4.7 Neural Synchrony

Normal cognitive operations require the transient integration of numerous functional areas widely distributed over the brain and in constant interaction with each other [30]. A hypothesis for this integration is the occurrence of neural synchronization. This phenomenon occurs on various levels of organisation of brain tissue, from individual pairs of neurons to larger scales and is mediated by neuronal groups that oscillate in specific bands and enter into precise phase-locking over a limited period of time [34]. The quantification of the level of synchronization between two signals originating from different regions in the scalp can thus provide a useful measurement of functional connectivity between two areas, or processes in the brain. This quantification is attempted through the calculation of Phase Synchrony Indexes (PSIs) through different methods. The following subsections describes some them.

#### 2.4.7.1 Coherence

One of the first methods for the study of the consistency between pairs of signals employed a method for measuring spectral covariance, traditionally referred to as frequency coherence (or Magnitude Squared Coherence (MSC)). It is a measure of the linear co-variance between two spectra. For each frequency,  $f$ , the MSC is defined for two zero-mean stochastic processes by the square of the absolute value of the cross spectral density [35].

$$c_{x_1x_2}(f) = \frac{|G_{x_1x_2}(f)|^2}{G_{x_1x_1}(f)G_{x_2x_2}(f)} \quad (2.10)$$



The spectra can be estimated from segments of the data by computing approximations using a DFT and averaging these across all segments. These segments are usually determined by a sliding window. The DFT provides a direct relationship between the time and frequency domains and represents the time difference as a phase difference or phase angle. If the time difference between two signals is stable and constant, then coherence equals unity. If this time difference varies from moment to moment then coherence equals zero. It is often interpreted as a measure of *coupling* and of the functional association between two brain regions.

Being a measure of the spectral covariance, the coherence result does not discriminate between effects of phase and amplitude in the interaction between two signals. To directly study the phase synchronization, tools where the phase component is separated from the amplitude are necessary. Another limitation of coherence is that it depends on the stationarity of the signal (as it relies on Fourier analysis), which is an assumption that can rarely be validated [36, 34, 30]. To cope with this, Lachaux et al. [36] devised a method for coherence measurement based on wavelet analysis. One last important drawback of coherence analysis is that the classical statistical analysis of coherence tests the null hypothesis that pairs of neural signals behave like independent white noise signals. As neural signals are not white noise, this hypothesis might be too strong and thus too easily rejected.

In the following subsections some more robust methods are presented, which enable the evaluation of synchrony in terms of phase and to some extent overcome the listed limitations of coherence.

### 2.4.7.2 Phase-Locking Value

As mentioned above, the classical method for estimating spectral covariance is valid only for stationary signals. Moreover, it is computed as a function of frequency and thus is sensitive to fluctuations in amplitude [37]. An alternative method to evaluate this relationship is by estimating the Phase-Locking Value (PLV). Since its introduction by Lachaux et al. (refer to [34]), this value became an important concept in dynamical and complex systems [37]. It uses responses to a repeated stimulus and seeks latencies at which the signals are phase-locked (the phase difference between them varies little across trials). Following the description in [34], given two signals  $x$  and  $y$  and a frequency of interest  $f$ , the first step is to apply a band pass filter to each of the signals in an

interval that contains  $f$ . Once this is done, the instantaneous phase of the signals is extracted. Lachaux used a complex Gabor wavelet centred at frequency  $f$ , but later studies successfully employed the Hilbert Transform and proved that the results yielded by both methods are similar [30]. In the context of the present text the use of the Hilbert Transform was adopted.

The PLV is then defined at time  $t$  as the average value

$$PLV_t = \frac{1}{N} \left| \sum_{n=1}^N \exp(j\theta(t, n)) \right| \quad (2.11)$$

here  $N$  is the size of the time series and  $\theta(t, n)$  is the phase difference  $\phi_1(t, n) - \phi_2(t, n)$ . The PLV thus measures the variability of this phase, within trials or in time. It takes values within the interval  $[0,1]$ , where 1 occurs when there is no phase difference between trials (or time intervals) - the signals are phase-locked. A null PLV indicates that there is no phase synchrony. Note that when  $PLV = 1$  the implication is not that both signals have an identical phase, but that the phases of both behave in a similar way.

Once the PLV is calculated it is necessary to apply a statistical analysis in order to differentiate significant PLVs against background fluctuations. Lachaux et al. introduced the Phase-Locking Statistics (PLS) method, which is detailed in subsection 2.4.7.4.

### 2.4.7.3 Phase Synchrony Index based on Entropy

Another commonly used method for quantification of synchrony is based on the concept of Shannon entropy [38].

The entropy,  $H$ , of the distribution  $P(\hat{\varphi})$  over  $N$  bins is given by:

$$H = - \sum_{k=1}^N P_k \ln(P_k) \quad (2.12)$$

where  $P_k$  is the relative frequency of finding the phase differences within the  $k$ th bin.

More specifically,  $\hat{\varphi}$  represents an interval, in this case a phase difference interval. Each bin is defined according to:

$$\hat{\varphi} = \hat{\phi}_1 - \hat{\phi}_2 \quad (2.13)$$

The maximum entropy of the signal is:

$$H_{max} = \ln N \quad (2.14)$$

$H \leq H_{max}$  unless  $P_k = k/n$  for all  $k$ .

The entropy index,  $\gamma$ , will be estimated by the expression:

$$\gamma = \frac{H_{max} - H}{H_{max}} \quad (2.15)$$

The entropy index is normalized to  $[0, 1]$ , where  $\gamma = 1$  implies that the signals exhibit exact rhythm locking and  $\gamma = 0$  indicates that there is no synchrony.

#### 2.4.7.4 Verification of the Significance of Phase Synchrony - Surrogate Tests

In the same paper they introduced the PLV, Lachaux et al., [34], suggested a statistical model to investigate the significance of the results. This method is based on the generation of surrogate data from the original series. The main advantage of this approach is that it does not require any a priori hypothesis about the signals. The null hypothesis ( $H_0$ ) that two series of phase values  $\phi_1(n)$  and  $\phi_2(n)$  are independent is tested.

The method consists in generating several surrogate time series by randomly shifting the elements of one of the original signals. For each surrogate series, the PLV between this and the original signal is measured, and used to evaluate the significance of the PLV between the original signals. The proportion of surrogate values higher than the original PLV returns the Phase-Locking Statistics (PLS) [34]: If the Phase Synchrony Index obtained for an original pair is greater than the level of significance ( $\alpha$ ) of the PSIs obtained for the surrogate series, the original pair is said to have significant synchrony.

This test can be extended to other PSIs, by substituting the PLV by the method of interest to calculate synchrony.



## 3 Objectives

The present chapter states the main goal of the thesis. Some studies that worked with BCI/EEG and stimulation in a feedback paradigm are presented. After this, some expected problems and the solutions found to deal with them are described. Finally, the general design of the desired system is outlined.

### 3.1 Main Goals

Most of the studies concerning tACS apply a preprogrammed stimulation signal. No feedback control is used in order to adjust the stimulation. The only adjustment is done manually after obtaining a baseline EEG from the subject in study. As was previously mentioned in the Fundamentals section, Section 2.2.2, tACS has been shown to improve cognitive function in humans when the stimulation is started in phase with the ongoing brain signal of interest (i.e., at the moment of stimulation both signals had the same instantaneous phase). This observation was made *a posteriori*, and this *in phase* start was not done in a systematic way. However, in a real life application, if one wished to improve cognition this cannot be attained by chance or approximation. Additionally, a system that enables a more controlled investigation of the interactions within the brain during and after the application of tACS would be of great use in the study of the brain dynamics, and of how the application of tACS influences them.

The seemingly obvious option is a feedback control system which determines the parameters of interest from the EEG signal of the user. This system would then produce a stimulation signal that is in accordance with the subject's individual brain activity. This needs, of course, to be done in real time. It is thus a natural leap to think of Brain-Computer Interfaces in this context, as the tools provided are standardized and readily available.

BCI has been previously used in conjunction with brain stimulation [39, 40]. In these studies, however, the type of stimulation was not tACS, but cortical stimulation, and the

aim was not to alter the stimulation parameters, but to condition the motor response to this stimulation.

The purpose here is not to alter the plasticity of the brain by conditioning responses, or to determine whether or not the subject fulfilled a certain task. The aim is solely to determine parameters from the spontaneous EEG (i.e., instantaneous phase and frequency), generate a stimulation signal, and start stimulation itself.

The ideal scenario is that in which the EEG is continuously read during stimulation and the parameters can be adjusted at any moment.

The following subsections explore the state of the art in the topic, some expected problems, and the planned design of the final system.

## 3.2 State of the Art

As mentioned above, BCI has been previously used in conjunction with cortical stimulation [39, 40], in a technique termed as Brain-State-Dependent Stimulation (BSDS). These studies by Walter et al. applied cortical stimulation to chronic stroke patients with right-sided hand paresis. The intent of the stimulation was to improve ipsilateral neural activity related to movement. The patients were implanted with an electrode grid that recorded the ECoG. The task was to attempt movement of the paralysed hand. This effort results in an Event Related Desynchronization (ERD) of the  $\mu$ -rhythm that, when detected, triggered an orthosis to open the paralysed hand and, at the same time, the application of cortical stimulation. Thus, the BCI system controlled the onset of stimulation, but it did not change any parameters. The first of these articles [39], studies techniques to remove stimulation after effects, such as artifacts and evoked activity, from the recordings, that could influence the detection of the brain states of interest.

Chen et al. presented a methodology based on autoregressive methods for the estimation of the instantaneous phase and frequency for phase locked stimulation [41]. These methods are applied to intracranial EEG at the *theta* band (4 to 8 Hz). The method relied on optimization of the passband, such that it would be narrow enough. However, such a narrow band filtering might result in an overestimation. The method performed well in artificial data, but was not as satisfying when applied to real EEG data.

Boyle and Fröhlich proposed an EEG feedback-controlled tACS stimulation system that controls cortical state dynamics [42]. For this, stimulation was applied occipitoparietally in the  $\gamma$  frequency band (40Hz), in response to endogenous  $\alpha$  rhythm activity

(stimulation was only applied when the detected  $\alpha$  had an amplitude above a determined value). It was observed that the  $\alpha$  frequency band was successfully suppressed for an eyes open paradigm. The study concludes that a feedback system is more effective than feedforward stimulation at controlling oscillatory dynamics in the  $\alpha$  band in the visual cortex.

Thus, there is evidence in the literature that such a system as is proposed here has a significant importance, and could be accomplished.

## 3.3 Anticipated Problems

### 3.3.1 Artifacts

As was mentioned in Section 2.2.2, the application of tACS is usually performed continuously over long periods of time. Ideally, the control of the parameters should be done during stimulation itself, thus creating an online feedback loop that could, in future applications, adjust the signal according to the observed parameters. However, the application of an alternating current over the scalp renders the measured EEG basically useless. The artifacts created are too intense to enable a reasonable treatment, that could result in a usable signal. Figure 3.1 represents a real case acquisition of EEG during a tACS session. During the five minutes of stimulation, the amplitude of the EEG rises to the point of saturation of the amplifier. As can be observed in figure 3.1b, the recorded signal acquires a quasi-sinusoidal shape, clearly influenced by the stimulation.

The amplifier used for acquisition of the EEG is thus a point to be considered. Some amplifiers can record signals with higher amplitude. If this range is enough for the amplifier to record the signal without reaching saturation, artifact removal techniques could be considered. In a recent study by Helfrich et al., [43], a method for reducing these artifacts is proposed. In this study, an artifact template was subtracted from every artifact segment using a moving average approach. The remaining artifacts were captured by Principal Component Analysis (PCA) and removed from the signal. There were some reservations regarding the methodology applied in the referred study. Specifically the fact that the group directly looked for a phase lock between the corrected signal and the stimulation (both at 10 Hz). According to the group, this is evidence of

### 3. Objectives

---

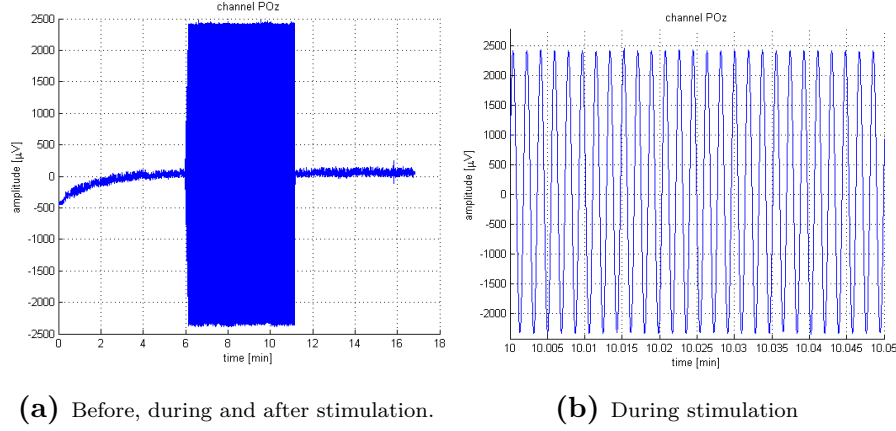


**Figure 3.1:** EEG recorded during tACS session. a) Recording before, during and after the application of the stimulation signal. b) representation of a segment of the EEG recording during stimulation.

entrainment, but it could also be an effect introduced by the artifact reduction method. Further verification should be made before applying this methodology in other research.

The study mentioned in the previous section by Walter et al. [39] that deals with after effects of stimulation for BCI use, is also not applicable in the present case, since the type of stimulation and resulting artifacts are very different. In the mentioned case, the artifacts were 30 ms long (induced by the stimulation). Between stimulation pulses there were 2 seconds of artifact free signal. The method basically consisted of cutting out the artifact, so that they do not influence the analysis of the signal. This solution is not applicable to the case of tACS, since it would result in a total absence of data to analyse (as there are no artifact free intervals between short periods of stimulation).

The artifact removal task is not trivial, and the efficacy of the methods is not known. As such, a deeper look into the problem should be taken separately, on a dedicated study.

For the work described in the present thesis, one of the available amplifiers saturated during stimulation, which made any attempts to reduce artifacts pointless. The second available amplifier that did not saturate was not compatible to the BCI2000 tools. Finally, the third available amplifier (g.USBamp from g.tec) was not tested for use with tACS, and, depending on the amplitude of the stimulation could very likely saturate. Thus, the problems associated with artifacts are avoided by studying the signals before and after stimulation, but not while it occurs. This is done under the assumption that



once the stimulation system is shown to work and the artifact problem is solved, it would be easy to apply a similar system in a continuous paradigm.

## 3.4 System Design

Usual tACS studies use rather long stimulation periods, spanning from a few minutes to more than thirty minutes of continued stimulation. For the purpose of the present work this would present a problem, since, due to the already discussed artifacts, it would not be possible to verify the fit of the stimulation. Thus, a first criteria that should be met in the experiments to be done in the context of the project is that the stimulation would need to be interrupted in cycles of some seconds to check and adjust the stimulation signal. The basic design of the system is explained below, and summarized in the diagram represented in Figure 3.2.

The EEG is recorded using a 16 electrode layout. The type of electrode to be used has to be tested for compatibility with tACS stimulation. The used amplifier is a g.USBamp from g.tec (details available at [44]). The output of the signal is connected to the working computer and read using BCI2000. Here the signals are analysed and the important parameters extracted. This step will implement one of the methods described and explored in Chapters 4 and 5.

Once the stimulation signal is determined, it will be generated using the sound card of the computer. The output signal is sent to the tACS stimulation device. This is a NeuroConn DC Stimulator Plus, with Remote option added. This option enables the external operation of the stimulator through a voltage supply source. The generated current follows proportionally to the applied voltage [45].

The stimulation is then applied for a duration of some seconds. The EEG is continuously acquired, but during this interval, it is not used. When the stimulation is stopped, the same procedure as in the beginning is performed, to detect whether or not this stimulation was done in phase with the signal. The intermission should be brief, lasting for around two seconds. The stimulation is then re-started, once again adjusted to the ongoing signal, for the same time interval. This should be repeated for some minutes.

Once the cycles are done, the EEG before and after stimulation should be analysed offline to assess if the approach was successful in achieving its main goal of starting the stimulation in phase with the ongoing brain signal.

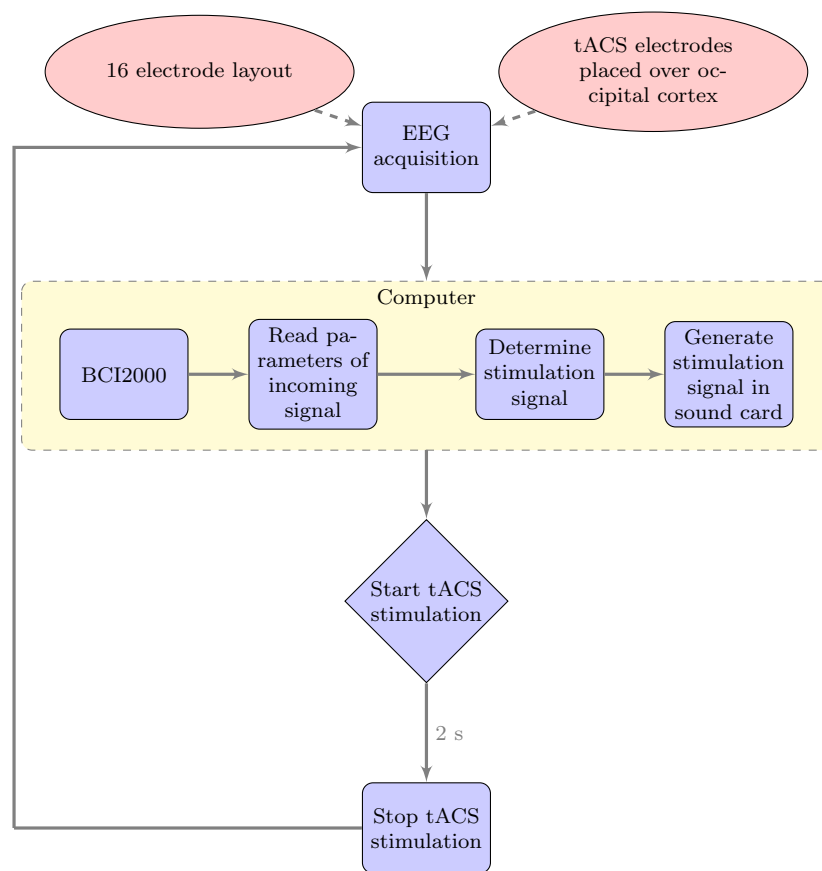


**Figure 3.2:** Basic design of the closed loop tACS/BCI system.

## 4 Methods

In order to initiate stimulation in phase with the ongoing EEG signal, an algorithm for phase detection and parameter setting of the stimulation wave must be selected. For this purpose, three different methods are devised, each based on a different premise, but all with the same background and purpose. This chapter presents the methods used for phase evaluation, the pre- and post-processing steps necessary for the analysis, and a description of the methods for generating the stimulation signal.

### 4.1 Phase Evaluation

For analysis of the phase, several methodologies are applied. For each of them, several intervals of the data are analysed. The methods described below are used within smaller segments of the main signal and are valid for use in a moving window analysis type or for analysis with no overlap. Since they are used in different paradigms, the details of how they are employed (in terms of windowing or segmentation of the original signal) for a particular application, are given along with the results.

#### 4.1.1 PLV

The phase-locking value was already extensively approached in the Fundamentals chapter, in particular in Section 2.4.7.2. Figure 4.1 represents two simple sine waves that undergo a PLV analysis. The phase series of each of the analysed signals is obtained by application of the Hilbert Transform. The difference at each time point between both is calculated, and applied to Equation (2.11) for determining the PLV.

$$PLV_t = \frac{1}{N} \left| \sum_{n=1}^N \exp(j\theta(t, n)) \right| \quad (2.11)$$

## 4. Methods

In the particular case of the signals represented in Figure 4.1, PLV will be equal to unity. As was described in section 2.4.7.2, the PLV reflects the average across the length of the analysed signals of the phase difference between them at each point. In other words, the PLV translates how the phase change in each of the signals relates to the other.

These PLVs are checked for significance using the Phase Locking Statistics (PLS) described in section 2.4.7.4.

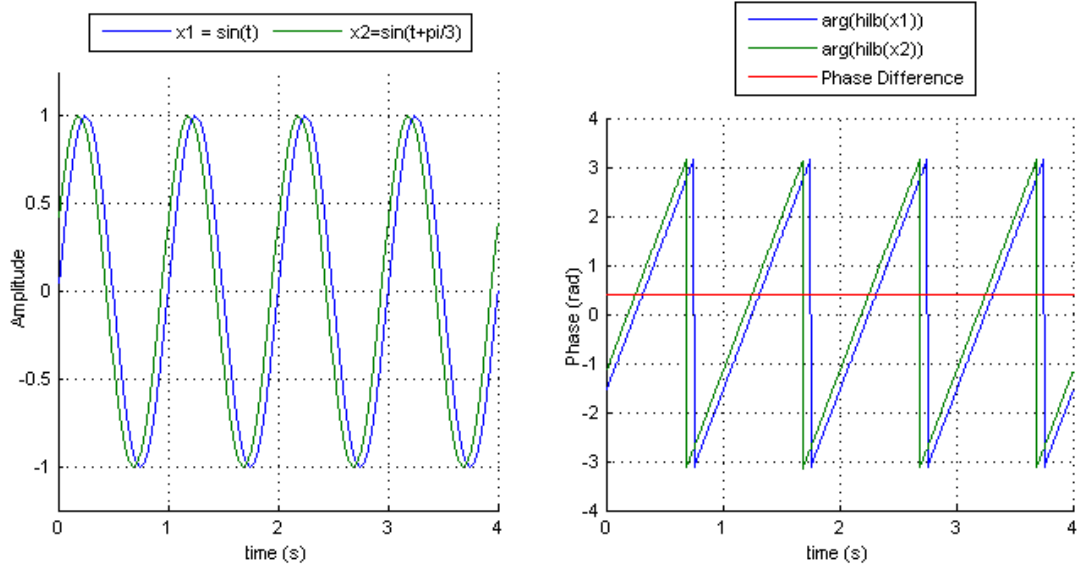


**Figure 4.1:** Illustration of the phase series resulting from the application of the Hilbert Transform. The instantaneous phase of the signals (right) is calculated from the Hilbert transform. Note that the application of the transform shifts the phase of the original signal by  $\pi/2$  rad. In this case, both signals are phase-locked, and have a constant phase difference of  $\pi/8$  rad.

### 4.1.2 Analysis of Histogram - Entropy

The series obtained by calculating the difference between the phase of two analysed segments is separated into bins. Each bin represents a phase interval. As such, it is possible to quantify how many points in the phase difference series fall into a certain phase. In the case of comparing two perfect sine waves, the resulting histogram is expected to center on one particular interval with possible outliers. When comparing

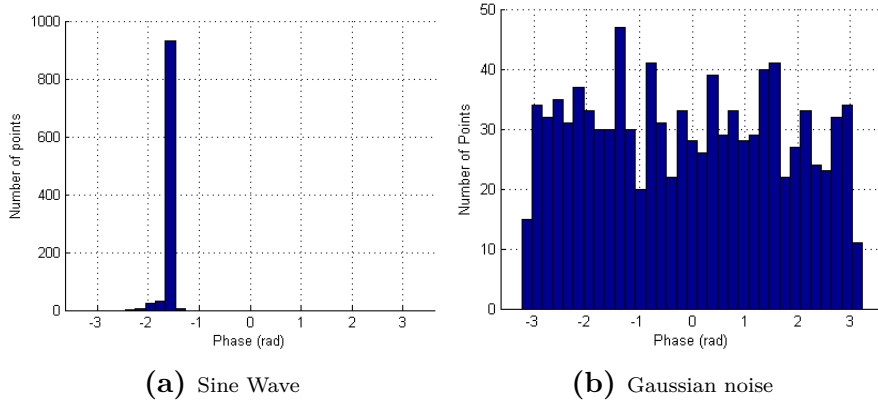


**Figure 4.2:** Example of distribution of the phase difference between two perfect sine waves (left) and two random signals (right). The distribution is represented in a  $[-\pi, \pi]$  histogram. Each bin represents a phase interval. The Shannon's entropy is calculated from the histogram.

some signal to a random distribution, the histogram is expected to span over all the bins. These two cases are depicted in Figure 4.2.

The entropy of this histogram can be calculated by use of the concept of Shannon's entropy  $H$  :

$$H = - \sum_{k=1}^N P_k \ln(P_k) \quad (2.12)$$

where  $P_k$  is the relative frequency of finding the phase differences within the  $k_{th}$  bin. Thus, a synchronization index  $\gamma$  as described in section 2.4.7.3 can be calculated.

$$\gamma = \frac{H_{max} - H}{H_{max}} \quad (2.15)$$

This index  $\gamma$  is calculated for the windows that comprise the signal. The results are represented in a plot of entropy index by analysed window, which will thus describe the evolution of the entropy index over time.

### 4.1.3 Peak-to-Peak Difference Analysis

The analysis of the phase is based on the instantaneous phase time series obtained by applying a Hilbert Transform to the original data signal. This new series usually has an almost sawtooth shape, as is illustrated in the signals in Figure 4.1. In a signal where the phase of the signals over time is stable, the distance between the peaks of the

sawtooth should remain constant. If the distance between these peaks is not constant over the length of the analysed signal, this is an indicator that the phase is alternating in a more or less erratic way.

This method thus simply consists of calculating the difference between peaks and verifying the variation over the length of the segment. In the case of a perfect sine wave, the result is expected to be a stable line, possibly displaying very slight variations. Since for a significant evaluation these results are averaged, and the peaks don't appear at the same moments in time, the X-axis in the plots is not time, but the number of the evaluated peak.

## 4.2 Algorithms for Closed-Loop Stimulation

### 4.2.1 Processing of Analysed Signals

**Band Pass Filtering over frequencies of interest** The analysis has to focus on a certain frequency band (in the present case  $\alpha$  band, approximately 10 Hz). It is then important to band pass filter the signal around this frequency.

In the case of the real signals, since there are several oscillators contributing to the signal, the central frequency might not be 10 Hz precisely, but only approximate it. Hence, it is important to know the central frequency,  $f$ , of the signal to make sure the filtering process is centred on this frequency. Since the band of interest is known, before calculating the power spectrum a zero-phase band pass filter should be applied around the frequencies of interest. That way a wider band than recommended for further analysis can be covered and adjusted afterwards. The power spectrum of the signal is then calculated, using the Welch method described in Section 2.4.3. For an EEG signal recorded over the occipital region at resting state and with eyes closed, the expected power spectrum approximates what is represented in Figure 4.3. The peak in this spectrum is defined as  $f$ .

Taking this into account, a Butterworth zero-phase filter is then applied at the frequency interval  $[f - 2, f + 2]$  (or a different one selected by the user).

An important remark is that this central frequency will be used to generate the stimulation signal. This follows the assumption that the central frequency of the signal of interest is constant and does not vary greatly along time [9].

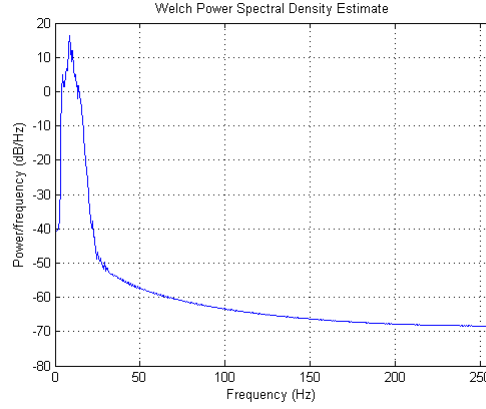


**Figure 4.3:** Application of Welch method for estimation of power spectrum. Applied to a signal recorded over the occipital region after using a bandpass filter between 6 and 14 Hz.

**Moving Window** To test the methods, the signals are divided into segments of a certain predefined length.

Within these segments, a first interval is selected, hereby termed reference. The methods are applied to this reference, and a stimulation signal is derived. A second, non-overlapping interval of the same length is used to adjust the stimulation signal. Finally, the analysis steps that are common to all methods are applied to a third interval of the same length. These intervals are represented in Figure 4.4.

The length of this interval determines the size of the window of analysis, which, as mentioned above, is the same for all the analysed intervals. This segment, constituted by three intervals of size *window*, is then advanced by a step of predefined length. The described procedure is repeated, and thus the final outcome of the analysis of the signal has a temporal continuity.

The size of the window can be adjusted, as well as the step advance by which the segment will be moved.

**Post-Processing of results** All the algorithms generate a stimulation signal. The same type of analysis is performed, making it possible to compare them. The PLV and corresponding surrogate tests (as described in Section 2.4.7.2), average and variance of phase difference are calculated for each segment. As mentioned above, this analysis is performed on the third interval of size *window*. As the segment is advanced, the final analysis will display the results of the tests over the analysed windows, which translate

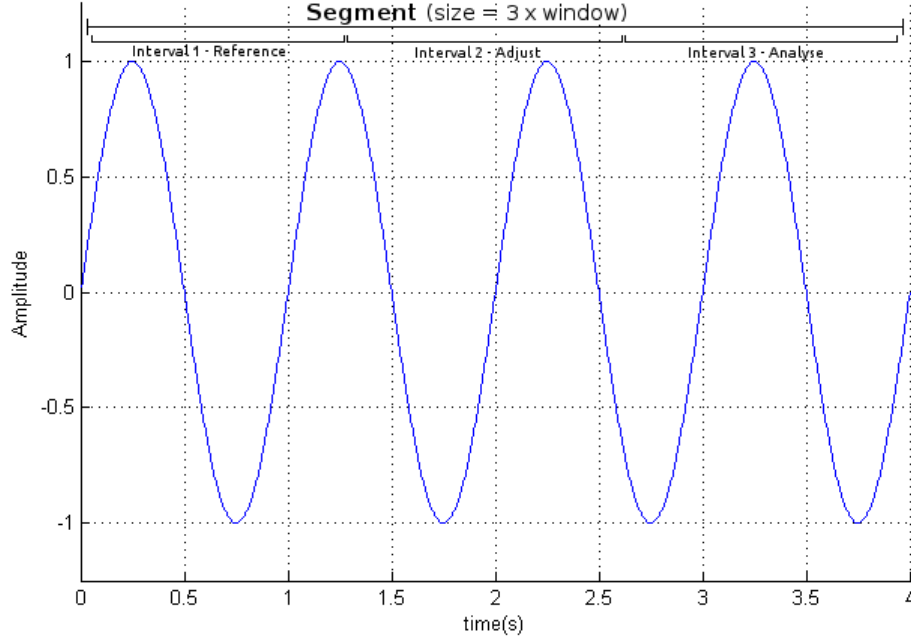


**Figure 4.4:** Representation of one segment and the defined intervals for application of the algorithms. This segment is constituted by three intervals of size *window*. The first interval is used as reference to generate the stimulation signal. The generated signal is compared to the second interval and adjusted if necessary. Finally, the adjusted signal is analysed against the third segment.

into a temporal advance. The stepping enables the advance to not be too fast, and thus a continuous analysis is simulated, where the phase detection would be continuously done and adjusted.

### 4.2.2 Method 1: Phase Shift Approach

The first algorithm is based on a *brute force* logic. After selecting the central frequency and defining the window and step lengths, several sinusoidal signals are generated with the phase varied in one degree steps. All the other variables are maintained constant. The PLV and phase difference are compared between each of these signals and the reference. The wave that presents higher PLV and lower phase difference is chosen as the stimulation signal.



### 4.2.3 Method 2: Adjustment Approach

The second algorithm attempts to determine the best phase by inspection of the original signal.

For this purpose, the instantaneous phase of the reference interval is calculated using the Hilbert Transform, as described in the previous section.

A sine wave is generated for stimulation with the same frequency as the central frequency of the original signal. The initial phase of this wave is defined as the instantaneous phase at the last point of the reference interval of the original signal, corrected by  $\pi/2$  radians, to account for the shift introduced by the HT (refer to Figure 4.5). Note that the segmentation and interval selection is again as represented in Figure 4.4.

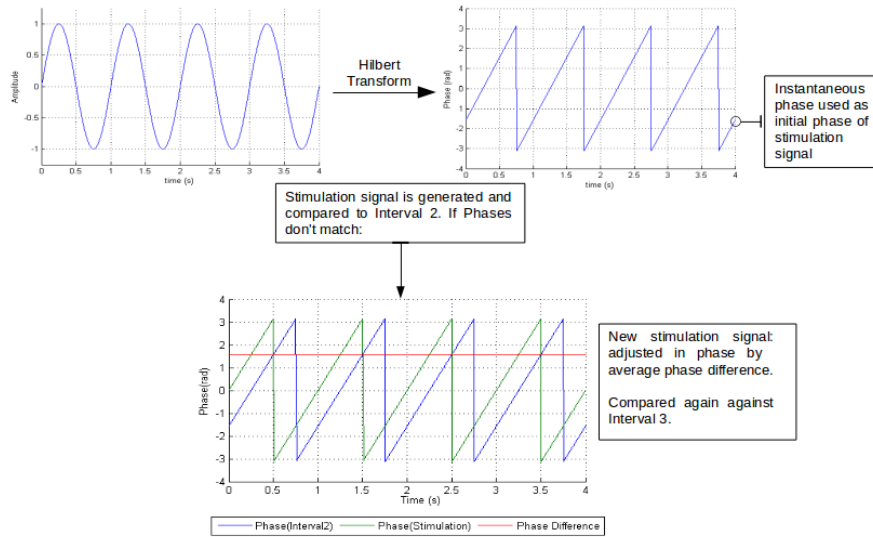


**Figure 4.5:** Illustration of the basic procedure used in the adjustment approach. The instantaneous phase is acquired from a reference interval, and a stimulation signal (sinusoidal) is generated. The initial phase of this signal is equal to the instantaneous phase at the last point of the phase time series, corrected by  $\pi/2$  radians. The generated signal is compared to a second interval; if the stimulation and the interval phases are still too different, the stimulation is adjusted. The final stimulation signal is analysed against a third interval, for evaluation of the method.

This signal is then evaluated in terms of phase, and compared using PLV and phase difference checks to the interval following the reference. At this point the phase difference corrected. For this purpose, the average of the phase difference over the interval is calculated and subtracted from the first generated signal.

Finally, the signal is compared to the third interval to evaluate the method.

#### 4.2.4 Method 3: Autoregressive Estimation of Reference

The third algorithm is based on the same adjustment principle as the previous method. Once the stimulation signal is determined, the steps are the same as described above.

The main and fundamental difference is the reference interval. In this case, an autoregressive model is used to estimate the phase of the signal at the moment of stimulation onset. Instead of using an interval retrieved from the original signal, the predicted signal is used as the reference interval (in the sense described previously). This predicted signal has a smaller size than the intervals defined in Figure 4.4.

For estimation of the reference, the Burg method [46, 47] with order  $p=4$  (variable when desired) is applied to the first interval of data to acquire the parameters of the model. Again, this interval is the same as defined in Figure 4.4. The second interval is used to estimate the signal, since if the same part of the signal from which the parameters derived was used, the estimation would over-perform. The equations in Section 2.4.5 are used. Figure 4.6 represents the estimated signal against the original signal (for a pre-processed simulated EEG signal consisting of two sine waves). The signal depicted in green corresponds to the estimated signal. After this step, the procedure is similar to Method 2. The instantaneous phase time series is calculated for this signal, and a stimulation signal is generated with initial phase retrieved from this series and again corrected for the  $\pi/2$  shift induced by the HT.

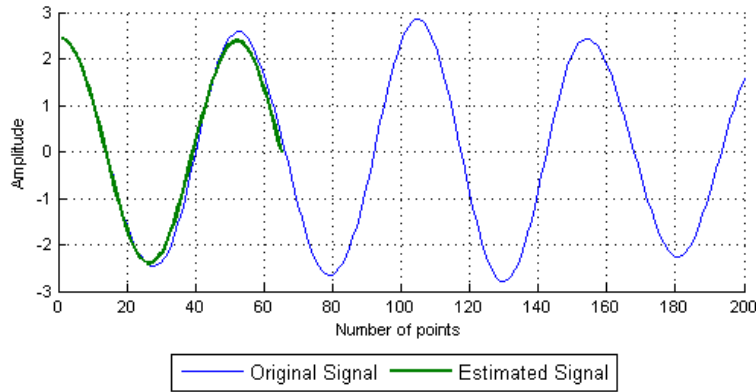


**Figure 4.6:** Time series predicted by AR estimation against the original pre-processed simulated EEG signal consisting of two sine waves. The signal depicted in green corresponds to the estimated signal. This estimation is used to acquire the predicted phase of the signal at the moment of stimulation.

## **4.3 Performance Evaluation of Algorithms**

### **4.3.1 Generation of Artificial Datasets**

For evaluation of the methods and analysis of the results, it is important to know what the behaviour of the methods is when signals with a known response are studied. Thus, three types of signals are generated: a simple sinusoidal signal, random noise following a Gaussian distribution (which approximates white noise), and a simulated EEG signal composed of one or more sinusoidal signals and added random noise. The noise was drawn from a standard normal distribution. For the simulation of EEG signals, a number of sine waves with adjustable parameters is generated (as many as desired). If there is more than one contributing sine wave, the waves are added and the root mean square of the result is calculated. To this new time series a certain amount of noise is added. The signal to noise ratio (SNR) is also user-defined.

### **4.3.2 Real Datasets**

For the evaluation of the methods and analysis of the phase itself, five datasets are available. The first one was recorded as part of the present work. The following four were acquired for BCI experiments, and present different characteristics. All the datasets were recorded by the BCI group at the University of Tübingen and made available for the present analysis by Dr. Martin Spüler.

#### **4.3.2.1 Recorded Dataset**

Three recordings were made as part of the present thesis. The recordings were taken from two different subjects.

One of the subjects performed two recordings: one with eyes open, and one with eyes closed. A 32 electrode layout with active dry electrodes in a 10/20 coordinate system based distribution (refer to Section 2.1) was chosen for the recordings. The amplifiers were two g.USBamp from g.tec. Common reference derivation was used.

The third recording was performed on another subject and with different recording settings. A 16 electrode display was used. The amplifier and type of reference reference were the same as before. The EOG was recorded for elimination of movement related artifacts. The subject was at rest, and had to open and close eyes upon cue.

The signals were filtered upon acquisition using a notch filter to attenuate power line interference and an additional band pass filter to exclude environmental noise.

Since there are only three recordings available, three to four channels of each recording are selected for analysis. All the used channels are located over the occipital area. This is performed to eliminate sporadic effects that could be connected to one specific channel.

### 4.3.2.2 Pre-recorded Datasets

**cVEP data** A dataset consisting of 45 EEG signals obtained for a code-modulated Visual Evoked Potentials (cVEP) based BCI is used for the analysis. The recordings obeyed a 10/20 coordinate system based distribution (refer to Section 2.1). Ground and reference electrodes were placed at FCz and Oz, respectively. The analysed channels are located above the occipital cortex. A more detailed description of the dataset can be found in [48].

**ErrP data** Acquired for the use of Error Potentials (ErrPs) for improvement of a P300 BCI. The dataset consists of 25 readings performed during a study of the increase of performance of a P300 BCI through the use of interaction Error Potentials (ErrPs). The recordings obeyed a 10/20 coordinate system based distribution (refer to Section 2.1). Ground and reference electrodes were placed at the left and right mastoid. The analysed channels are located above the occipital cortex (Oz position). For more information about this dataset refer to [49].

**Vigilance data** The database consists of three very long recordings obtained for a vigilance experiment. Here the task was to stay awake during a tedious observation task. The channels used for analysis are located on the occipital area. There is no available information about the exact montage.

**ECoG data** This dataset is composed of five ECoG recordings acquired for a study on stroke rehabilitation coupling BCI and cortical stimulation. The recordings were obtained using a 16 electrode grid over the pre-motor cortex. Here the channel used for analysis is located over the pre-motor cortex.  $\mu$  rhythm is analysed in this case. For more details on the dataset refer to [39].

# 5 Results

In the present chapter, the results regarding the application of the methodologies described in Chapter 4 are presented. The algorithms for phase detection and stimulation setting are first tested and then applied to real data. At this step, a problem was detected regarding the analysis of the real phase, for which reason the second half of the chapter deals with the problem of analysing the stability of phase in real signals for short time intervals.

## 5.1 Algorithms for Closed-Loop Stimulation

Regarding the methods for stimulation adjustment, the first important step is to test them in artificial datasets. After a proof of concept regarding the methods is achieved, the optimal size of the analysed window and shift advance is selected, and the best of the three methods chosen. The next step is then to apply this method to a real set of data.

### 5.1.1 Algorithms in Artificial Datasets - Proof of Concept

In order to evaluate the algorithms exposed in section 4.2, each of the methods was run for two different types of generated data: sine wave and random Gaussian noise. The expected behaviour is, for the case of the sine wave, a constant PLV of value one, and a phase difference of zero for all analysed windows. Gaussian noise should yield the worst possible outcome: a very unstable PLV and phase difference are expected. The method is run for 20 signals of each type, and the results displayed are averaged over all of them. These datasets were run for a moving window of size 512 points, with an advance step of 64 points.

## 5. Results

Average over Windows (Sine Wave)	Method 1	Method 2	Method3
PLV	1.0000	1.0000	1.0000
PLS	0.0000	0.0000	0.0000
Phase Difference	0.0008	0.0007	0.0009
Standard Deviation of Phase Difference	0.0005	0.0003	0.0003
Average over Windows (Gaussian noise)	Method 1	Method 2	Method 3
PLV	0.455	0.456	0.455
PLS	0.012	0.010	0.011
Phase Difference (rad)	0.567	1.516	1.572
Standard Deviation of Phase Difference	1.046	0.785	0.765

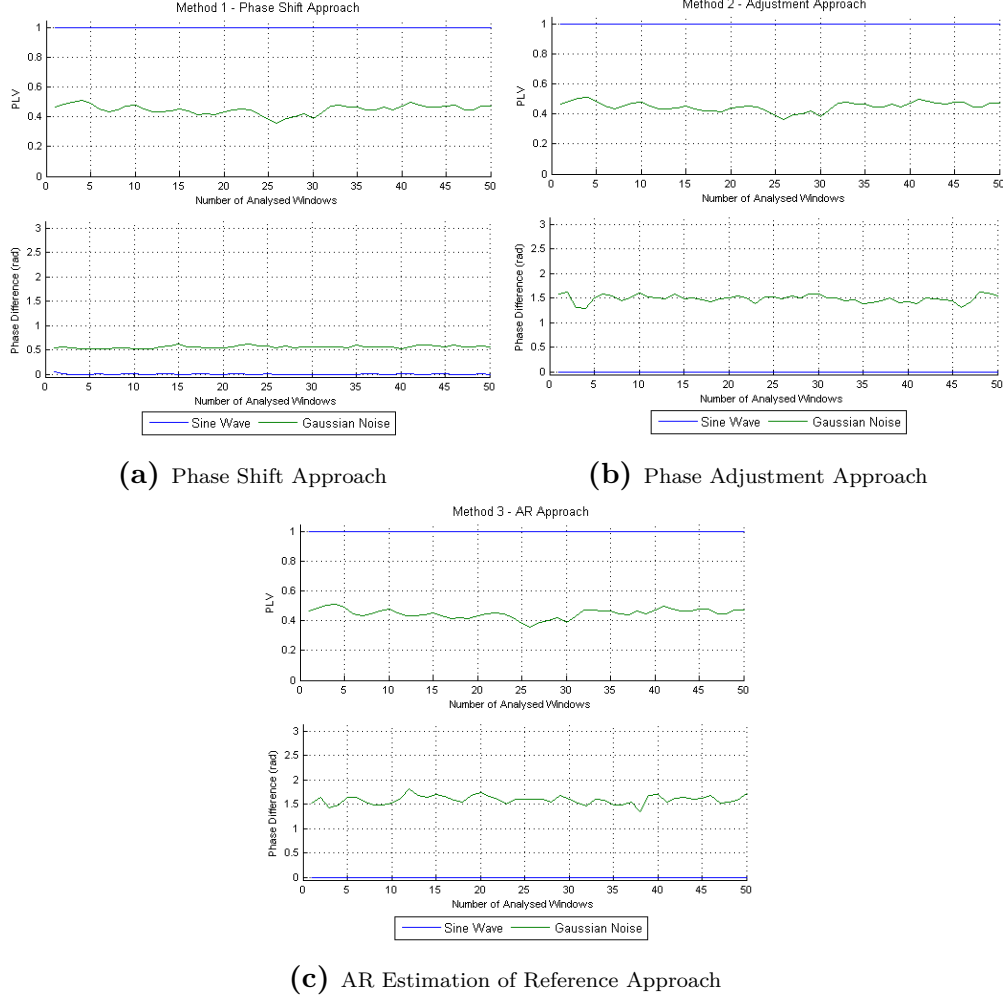
**Table 5.1:** Average values of PLV, surrogate alpha test, phase difference and its standard deviation for sine waves (top) and Gaussian noise (bottom), for each method.

Table 5.1 displays the average PLV and phase difference over the analysed windows for the dataset. The average for each of the windows for both sine and noise signals are plotted in Figure 5.1. The results yielded are as expected. In the case of Method 1 (Phase Shift Approach - PSA, Fig. 5.1a), the phase difference of the noise signal presents a lower value across all the windows. However, this is accompanied by a very high standard deviation and a PLV value equal to the one obtained with the other two methods. This indicates that the method is able to approximate, in average, the phase of even unstable signals, but the instantaneous phase of the stimulation signal does not, for which reason there is no phase-lock.

### 5.1.2 Selection of Size of Window and Step Interval

The next important step is to select the size of the window and step advance for the moving window analysis that yields the best results. Method 2 (Phase Adjustment Approach - PAA) is chosen for the analysis due to its computational efficiency, and under the assumption that in the extremes all three methods should show similar behaviour (with Method 3 being expected to decrease performance for long windows). The results for simulated EEG were chosen for display, since they have a known behaviour, but do not yield perfect case results, as in the case of the sine wave.

The algorithm was run for several window sizes, and for each of these windows for increasing step advance intervals (from 32 points to the same size as the window - no overlap). PLV and phase difference results were calculated. The average over the measured windows for each combination when analysing simulated EEG signals is



**Figure 5.1:** Methods for generation of stimulation signal: proof of concept. Each method is run for a group of sine waves and Gaussian noise. The signals are analysed with a moving window of 512 points with a step advance of 64 points. For each method PLV (top) and average phase difference (bottom) for each analysed window are represented. The sine wave results are represented in blue; Gaussian noise results are shown in green.

## 5. Results

displayed in tables 5.2 and 5.3. An important note is that this study of window size may differ according to the sampling frequency of the analysed signals. In the present case, the simulated EEG signal used has a sampling frequency of 512 points per second.

**Comparison of phase difference results when varying the size of window and step advance. - Simulated EEG signal**

Size of step	Size of Window							
	32	64	128	256	512	1024	2048	4096
32	2.332	0.785	2.818	1.459	1.427	1.348	1.243	1.077
64	-	1.278	1.080	<b>0.112</b>	<b>0.103</b>	<b>0.100</b>	<b>0.096</b>	<b>0.098</b>
128	-	-	2.675	0.133	<b>0.130</b>	<b>0.132</b>	<b>0.132</b>	0.134
256	-	-	-	0.191	0.176	0.181	0.193	0.222
512	-	-	-	-	0.180	0.174	0.183	0.212
1024	-	-	-	-	-	0.191	0.182	0.209
2048	-	-	-	-	-	-	0.179	0.193
4096	-	-	-	-	-	-	-	0.214

Size of step	Standard Deviation				
	Size of Window				
	256	512	1024	2048	4096
64	0.0458	0.0326	0.0225	0.0125	0.0070
128	0.0610	0.0484	0.0431	0.0381	0.0378

**Table 5.2:** Phase difference for different window and step advance combinations. The step advance varies from 32 points to size of window, in which situation there is no moving window analysis. The best results are emphasized. The lower table shows the standard deviation of this average phase difference for the highlighted values.

From inspection of tables 5.2 and 5.3 it is possible to infer that the ideal is to have a large window, which is shuffled by a small step. The interval that produces lowest average phase difference and a still small standard deviation occurs for a window of 2048 points (corresponding to 4 s) with a step advance of 64 points (corresponding to 0.125 s). However, this combination produces a high computational load, that is not optimal for real time application of the method. Besides, the available window on BCI2000 corresponds to 2 seconds. In the case of the simulated signal (and real signals used for method analysis) the sample frequency is 512 points per second, which means that the window should not exceed 1024 points (2 seconds). The standard deviation for the highlighted values in table 5.2 are also the smallest, indicating that the calculated phase difference is rather stable over analysed windows. If PLV analysis is also taken into account, it is possible to see that medium sized windows (256 to 1024 points) provide



Comparison of PLV results when varying the size of window and step advance. - Simulated EEG signal								
Size of step	Size of Window							
	32	64	128	256	512	1024	2048	4096
32	0.9365	0.9545	0.9821	0.9967	0.9951	0.9942	0.9938	0.9934
64	-	0.9436	0.9587	<b>0.9967</b>	<b>0.9951</b>	<b>0.9942</b>	0.9938	0.9934
128	-	-	0.9900	<b>0.9967</b>	<b>0.9951</b>	<b>0.9942</b>	0.9938	0.9934
256	-	-	-	<b>0.9965</b>	<b>0.9950</b>	0.9942	0.9938	0.9934
512	-	-	-	-	<b>0.9951</b>	0.9942	0.9938	0.9934
1024	-	-	-	-	-	0.9942	0.9938	0.9934
2048	-	-	-	-	-	-	0.9937	0.9934
4096	-	-	-	-	-	-	-	0.9934

**Table 5.3:** PLV for different window and step advance combinations. The step advance varies from 32 points to size of window, in which situation there is no moving window analysis. The best results are emphasized.

the best results. These results were checked using the surrogate method described in Section 2.4.7.4. The resulting PLS were zero for all combinations, which indicates the PLV is significant.

However, a real signal is expected to show more variance than the simulated EEG. Thus, a two second long window might prove too long, especially when it comes to comparing the signals upon start of stimulation. Thus, further comparison should be made between a combination of window size 256, 512 and 1024, and step advance of 64 and 128. The results of Method 2 for these combinations are plotted as PLV and phase difference over analysed windows. This is represented in Figure 5.2. Since the average values are known, the plots represent only the values in a small amplitude interval, in order to better observe small variations.

There is a high interest in observing a more or less constant result over the analysed windows, both for phase difference and PLV. This would indicate that the output of the method is consistent along the analysed segments.

From Figure 5.2, it is possible to see that a higher step advance produces a more variable phase difference. This step advance indicates that there is a higher time difference between the analysed windows. Such an increase in variability makes the evaluation of the method more difficult, and as such, a smaller step advance is preferred.

Regarding the PLV a slight difference exists when comparing window sizes: a smaller window yields a more variable PLV. This is not as pronounced as in the case of phase difference, though. However, considering the real situation, the best option is to select

## 5. Results

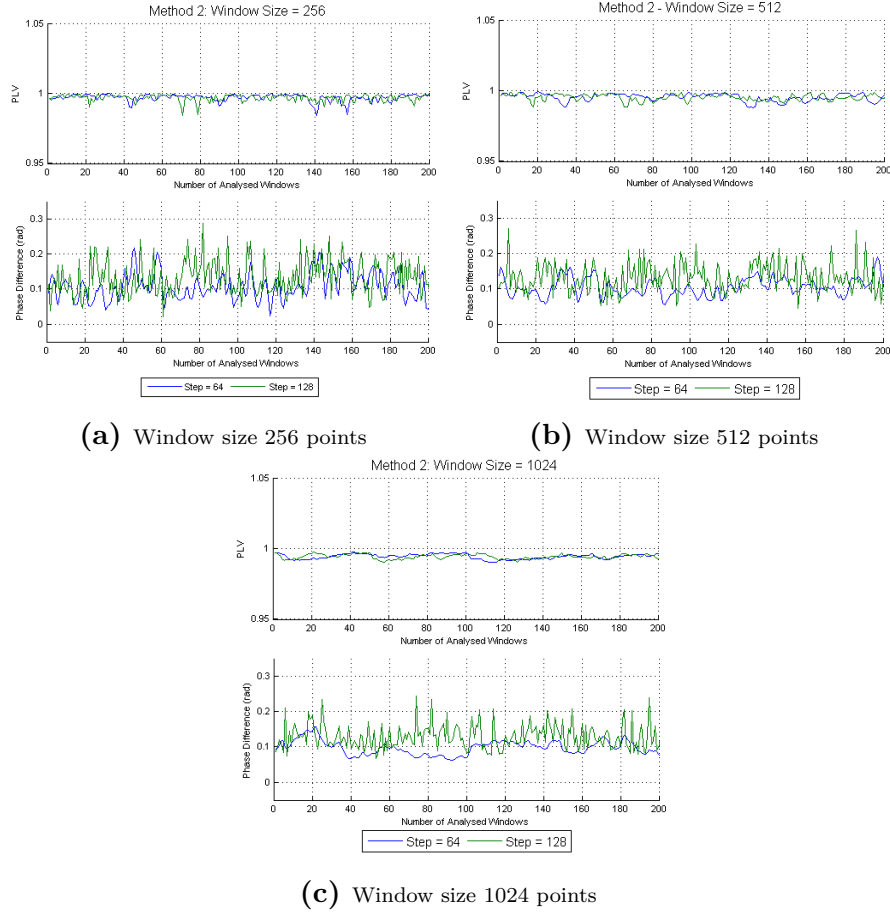


**Figure 5.2:** Comparison of PLV and phase difference over analysed windows for different window and step interval sizes. This comparison contemplates only Method 2 (Phase Adjustment Approach) applied to simulated EEG data. a) window size is 256 points, and step advance is 64 (blue) and 128 (green). b): window size is 512 points, and step advance is 64 (blue) and 128 (green). c): window size is 1024 points, and step advance is 64 (blue) and 128 (green). The results are averaged for a group of 10 simulated EEG signals.

a window size of 256 points with step advance of 64 points, as it would translate into a reference, and comparison windows of 0.5s (for a sampling frequency of 512 points per second).

### 5.1.3 Selection of best Method

For a real time application it is important to choose the method which offers the best compromise in performance, complexity and computational load. In order to compare the algorithms, each of them is applied to three different datasets: sine waves, random Gaussian noise and simulated EEG. Each group is constituted by ten signals. The output of each method for a certain group is averaged along trials for each analysed window (Figure 5.3). Table 5.4 lists the average over all analysed windows for the simulated EEG dataset of: PLV and corresponding PLS, phase difference, standard deviation, and elapsed time for computation <sup>1</sup> (including the analysis) of one signal.

Average over Windows (Simulated EEG)	Method 1	Method 2	Method3
PLV	0.997	0.997	0.997
PLS	0.000	0.000	0.000
Phase Difference	0.063	0.110	0.109
Std of Phase Difference	0.037	0.053	0.053
Time <sup>1</sup> (s)	62	6	305

**Table 5.4:** Average values of PLV, surrogate alpha test, phase difference, its standard deviation and computational time for each method. Results displayed for Simulated EEG.

Through observation of Figure 5.3 and Table 5.4, the three methods seem to have similar outcomes. In fact, for the same dataset all three yield the same PLV results. Regarding phase difference, the Phase Shift Approach (Method 1) presents a more stable output, even in the case of Gaussian noise. This implies that the method is able to follow the original signal in a more accurate way, but, as was seen by the results in Section 5.1.1, it approximates the results in average, and not when considering the instantaneous phase. Moreover, a small phase difference combined with a low PLV is meaningless. On the other hand, when comparing simulated EEG signals all methods yield similar phase differences. Thus, considering that both Method 1 (Phase Shift Approach) and Method

---

<sup>1</sup> The results were obtained using an Intel® Core™ i5-2410M CPU @ 2.30GHz, and 4GB of RAM running Matlab™ 32 bit on Windows 7. The elapsed time serves merely as a comparative parameter, and is not representative.

## 5. Results

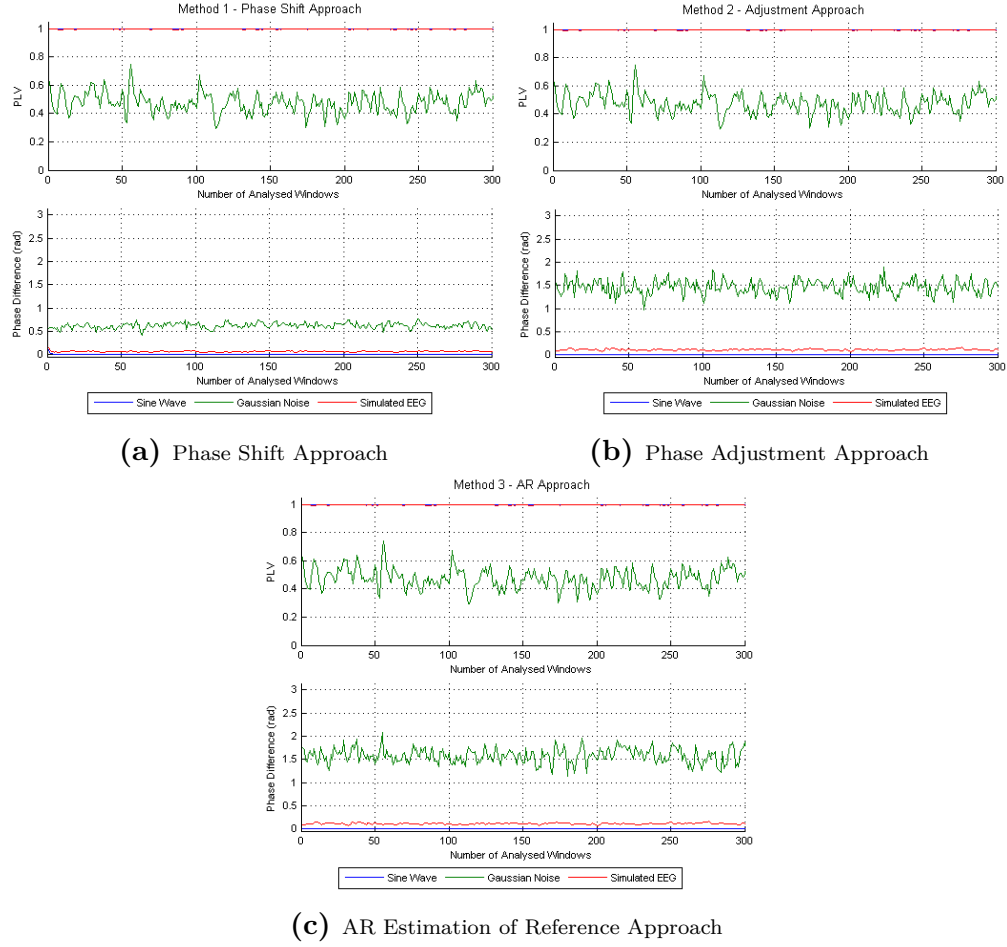


**Figure 5.3:** Comparison of the outcome of the three methods. The analysed data was composed by three groups of artificial data: simple sine wave, Gaussian noise and simulated EEG. Each group was comprised of 10 different signals. The represented signals are averaged for each of the groups. window=512; step=64.

3 (Autoregressive Estimation of Reference Approach) have much higher computational times and don not yield considerably better results, the best method for further use is Method 2 (Phase Adjustment Approach).

#### 5.1.4 Application of selected Method to real data

The Phase Adjustment Approach (PAA) method is applied to the dataset of real EEG signals described in Section 4.3.2.1.

As was done in the previous subsection, the output of the method is averaged over the analysed windows. The outcome is represented in Figure 5.4.

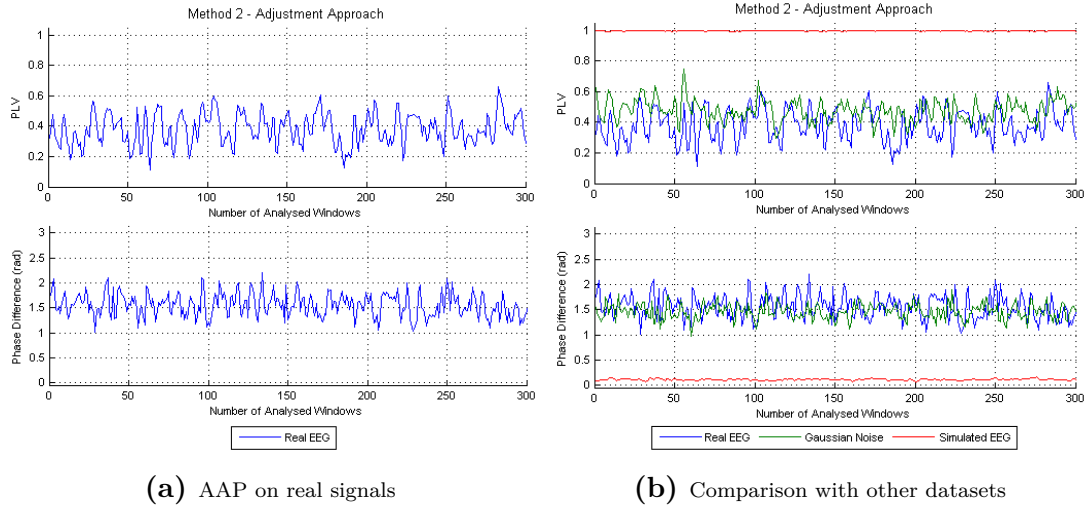


**Figure 5.4:** Phase Adjustment Method applied to real signals. In b) the outcome is compared to the simulated EEG signal and Gaussian noise outcomes using the same dataset as in the previous subsection 5.1.3. Note that both the PLV and phase differences results show a very similar behaviour to that seen for the noise signals.

The outcome of the method is not what would be expected. Both the PLV and the phase difference between the generated stimulation and the original signals resemble the results obtained for noise signals. Table 5.5 compares the average results over the analysed windows for real, noisy and simulated EEG signals. Again, it is possible to observe that the results for Gaussian noise and the real signals are similar.

In order to evaluate the stability of the intrinsic EEG phase, a detailed analysis of real sets of data follows.

## 5. Results

Average over Windows (Method 2)	Simulated EEG	Gaussian noise	Real Signal
PLV	0.997	0.489	0.388
PLS	0.000	0.030	0.151
Phase Difference (rad)	0.110	1.452	1.579
Standard Deviation	0.053	0.749	0.768

**Table 5.5:** Comparison of the average values of PLV, phase difference and standard deviation over the analysed windows for real, noisy and simulated EEG signals.

## 5.2 Analysis of Phase Stability

In order to analyse the phase of the signals, the methods described in Section 4.1 are here applied to different datasets of real data. Before this, the stability of simulated EEG signals with different numbers of composing oscillators is tested. The aim is to verify whether the number of contributing oscillators plays an important role in the instability of the phase of the signal.

The first group of real data is compared to all the other generated data (the same as used in the previous section), to get an idea of the expected distribution. The following subsections compare the other real datasets to Gaussian noise.

### 5.2.1 Influence of Number of Contributing Oscillators on Simulated EEG Signals

Using the method described in Section 4.3.1, several simulated EEG signals were generated. Ten groups of 30 signals each were defined. Each of these groups was composed of signals with a different number of contributing oscillators. All the sine waves used had a frequency close to 10 Hz, and a randomly chosen initial phase. Noise was added with a constant SNR. The signals are analysed over consecutive segments of six seconds. The PLV is calculated for a selected reference window of one second, against a moving window of the same size, that is shifted by 0.25 seconds, until the end of the segment. With this type of analysis, the PLV should yield a measure of the stability of the signal along the analysed segment. The distance between consecutive peaks (the peak-to-peak difference) is also verified. Figure 5.5 represents the average peak-to-peak difference for each group, and the PLV calculated over all the segments regarding each type of simulated signal (from one oscillator to ten).

These results point in the direction that the stability of the phase of the simulated signals varies with the number of oscillators that contribute to it. However, this variation

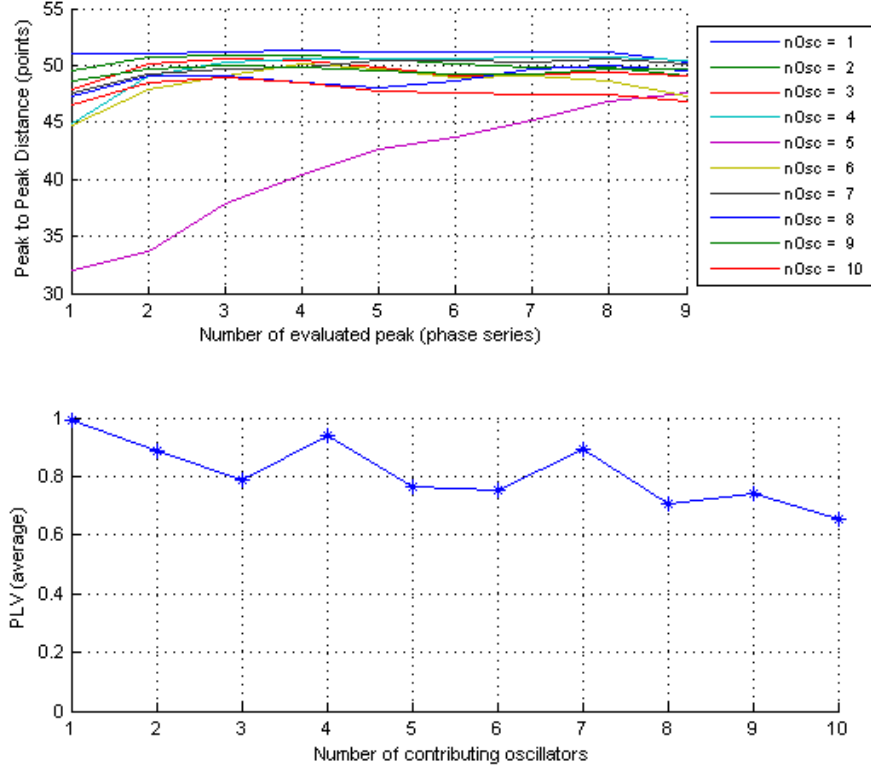


**Figure 5.5:** Peak-to-peak distance (top) and PLV (bottom) averaged across analysed segments of simulated signals according to the number of contributing oscillators. For each type of contributing oscillator number, 30 signals were generated and analysed.

is not linearly related to the number of oscillators. Figure 5.5 shows the evolution of the average PLV according to the number of oscillators considered for simulation of the real signal. As can be observed, this value seems to slowly decrease in average, but this is not attained linearly. In fact, the plot indicates that a simulated signal with two oscillators will yield similar results to a simulated signal composed by the mixture of seven oscillators. Looking at the peak-to-peak difference plot, it is possible to observe that the distance between peaks remains approximately constant, except for the case when the number of contributing oscillators is five. Excluding this result, it would be possible to infer that the number of oscillators does not have a significant influence on the stability of the simulated EEG. Thus, two contributing sine waves will yield results not far from if the ones obtained when more oscillators are used.

### 5.2.2 Comparison of Different Signal Types (Artificial and Real)

Using the same datasets as in Sections 5.1.4 and 5.1.3, PLV, peak-to-peak difference analysis, average phase difference and entropy analysis were applied. The average distribution of these measures for each dataset are compared in Figure 5.6. Each of the analysed segments is averaged over the entire group.

The signals are divided into segments of a determined length, typically with a duration of six to ten seconds. The peak-to-peak difference is calculated across the entire segment. For the other methodologies, each of the segments is tested for stability according to a moving window paradigm: a first section of the segment, of length  $x$ , is set as the reference window. This window is shifted in  $y$  sized steps, and the PLV and synchrony index are calculated between the advanced windows and the original one. This will enable the analysis of the evolution of these values along the segment. These segments are finally averaged for the entire signal.

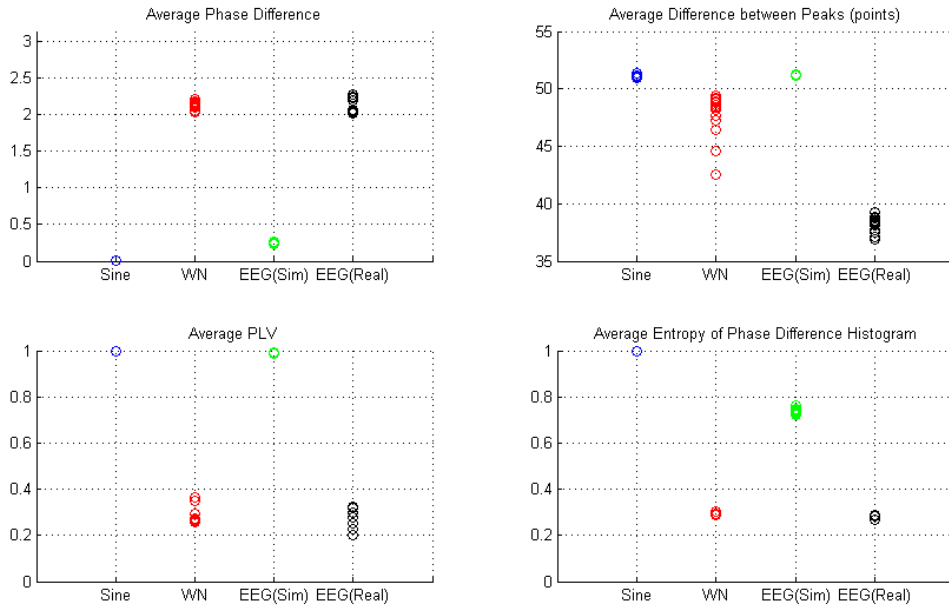


**Figure 5.6:** Comparison of the average values of mean, peak-to-peak difference, PLV and synchrony index for each signal contained in the dataset. The set consists of groups of ten time series each of: sine waves, white noise, simulated EEG and real EEG. Window = 2s; Step = 0.5s.



In terms of peak-to-peak difference, the average distance in itself does not carry valuable information. The variability of the results is the most important. In this scope, it is possible to observe that the average for real EEG signals presents a high variability. Both PLV and synchrony index are low and variable in average for the real signal, being comparable to the noise time series.

In order to investigate how this translates in a more general case, it is necessary to analyse more datasets for real signals. This is done in the following subsections, and the results are compared to the case of random signals over a normal distribution (again, Gaussian noise).

### 5.2.3 Comprehensive Analysis of Different Datasets

The methodologies described in Section 4.1 are applied to the datasets described in Subsection 4.3.2.2. Each of the datasets is compared to Gaussian noise signals. The set of noisy signals is adjusted, so the number of analysed series is the same for the real and noise datasets. Note that the noise datasets are not the same for each analysis.

#### 5.2.3.1 cVEP Data

The idea here is that upon presentation of a visual stimulus of determined frequency the EEG will elicit an evoked potential at the same frequency as the stimulus. The currently accepted hypothesis concerning this regulation is that a phenomenon of *phase resetting* happens in this moment [50]. As the name suggests, the phase of the brain signal changes, and thus the frequency is also adjusted. It is thus expected that in the interval between phase resetting events the phase of the signal is stable, since the frequency is assumed to remain constant in this interval.

As such, the previously demonstrated methods for phase analysis are applied to this interval. In the case of the present dataset, there is an interval of 1.05 seconds between presentation of stimulus. The sampling frequency is 600 Hz. The stimulus has a duration of 0.06 seconds. This interval and the following 0.06 seconds are excluded from the analysis. A window of one quarter of the length of the interval is used as reference. This reference is compared to a second window that is advanced at a step of one quarter of the size of the reference. Thus, the first window of comparison evaluates the reference window against itself. The same type of analysis is performed for Gaussian noise.

## 5. Results

To test the results of the analysis of real data against Gaussian noise, a two sided Mann Whitney U-test test is applied to the averaged results along the datasets. The aim is to test the null hypothesis,  $H_0$  that the medians of the signals are the same, against the hypothesis that they are not. The results are compared in Figure 5.7 and Table 5.6.

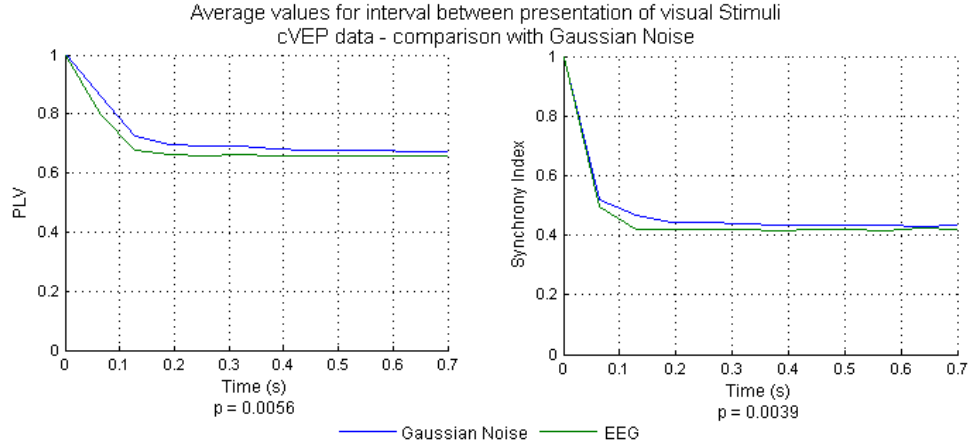


**Figure 5.7:** PLV and synchrony index for cVEP data. Average along the time between presentation of stimulus for the complete dataset. The  $p$ -values resulting of the application of the Mann Whitney U-test to the average values against Gaussian noise are listed under the plots.

	Gaussian noise	Real EEG	$p$ -value (2 sided)
Phase Difference	1.940	1.960	0.862
Standard Deviation of Phase Difference	1.163	1.162	0.326
PLV	0.727	0.700	0.006
PLS	0.011	0.012	-
Synchrony Index	0.493	0.474	0.004

**Table 5.6:** Average results of stability tests for cVEP data and respective  $p$ -values resulting from the application of the Mann Whitney U-test to the average values against Gaussian noise.

For the PLV and synchrony index there is evidence that the medians of the signals are not the same ( $p$ -value is lower than  $\alpha = 0.05$ ); the null hypothesis  $H_0$  can be rejected. By graphical inspection it is possible to observe that the the average PLV of the Gaussian noise is higher than the one of the real signal. The PLV value for both EEG and white noise is very high, and according to the PLS, it is significant. This might derive from the fact that the analysis is done over a very small window, and for small segments. The

comparison with Gaussian noise invalidates a conclusion that the real signal presents phase stability (since Gaussian noise is known to be random).

### 5.2.3.2 ErrP Data

The analysis is performed using the same paradigm as described above (Section 5.2.2) for the comparison between different datasets. Here, the most interesting results are for peak-to-peak difference and PLV. The results regarding the PLV were tested using a surrogate test, consisting of 39 surrogate series. The resulting level of significance was inferior to the defined threshold of  $\alpha = 0.05$ , which means they are significant.

The analysis was performed using the same moving window paradigm described in Subsection 5.2.2. The segments had a duration of five seconds, the window length was defined as 0.5 s and the step size 0.125 s. The peak-to-peak difference was calculated over the length of the segment, and is displayed by number of analysed peak. The results regarding peak-to-peak difference and PLV for the first two seconds of the segment are displayed in Figure 5.8, and the average values are listed in Table 5.7.

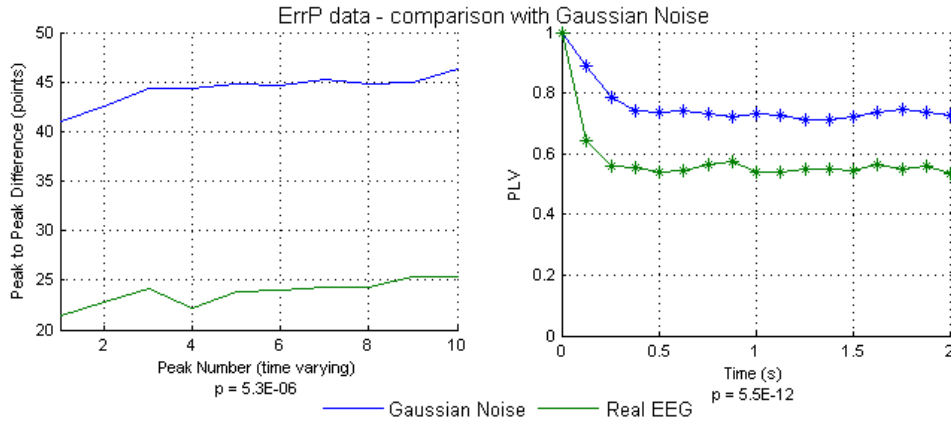


**Figure 5.8:** Peak-to-peak difference and PLV for ErrP data. Average along segments (peak-to-peak difference: non-overlapping; PLV: overlapping). The  $p$ -values resulting of the application of the Mann Whitney U-test to the average values against Gaussian noise are listed under the plots.

By inspection of Figure 5.8 and Table 5.7, it is possible to observe that there is a clear distinction between Gaussian noise and EEG signals. The null hypothesis  $H_0$  that both types of signals have the same median can be rejected, as the  $p$ -values obtained from the two sided Mann Whitney U-test are significantly lower than the threshold

## 5. Results

	Gaussian noise	Real EEG	$p$ -value (2 sided)
Phase Difference	2.054	2.040	0.471
Standard Deviation of Phase Difference	1.217	1.317	2.821E-02
PLV	0.740	0.558	5.479E-12
PLS	0.011	0.029	-
Synchrony Index	0.475	0.391	5.479E-12
Average Peak-to-Peak Difference	44.680	24.192	5.331E-06

**Table 5.7:** Average results of stability tests for ErrP data and respective  $p$ -values resulting from the application of the Mann Whitney U-test to the average values against Gaussian noise.

$\alpha = 0.05$  value. However, the average values of the PLV and the synchrony index are lower for the EEG than for the Gaussian noise, indicating less phase-lock. Thus, despite showing that the behaviour of the real EEG signals is not equal to Gaussian noise, it is not possible to find any evidence to support the existence of stability in the phase of the EEG.

### 5.2.3.3 Vigilance Data

The signals considered in this analysis are very long. Due to the nature of the experiment from which they were recorded, there may be some phase resetting events present. However, the large number of considered segments should be enough to enable the detection of stability if it exists. The advantage of this set is that the length of each recording enables the analysis of a very high number of segments. Potential deviations and noise are expected to be minimized when averaging.

As in the previous dataset, the analysis paradigm followed the one described in Section 5.2.2, and the PLV values were tested for significance using a surrogate test. The analysis was performed for a window of length 0.5 s and step size 0.125 s, over a five second segment. The peak-to-peak difference was calculated over the length of the segment.

Regarding the peak-to-peak difference analysis, the EEG signal follows a pattern very similar to the one observed for Gaussian noise. The  $p$ -value obtained by the application of the Mann-Whitney test is significantly inferior to the threshold  $\alpha = 0.05$ . This indicates that the average distance between peaks is distinct between the signals, and thus one can infer that the behaviour of the real signal is not similar to Gaussian noise. This is in fact supported by evidence that the PLV does not have the same median for real and noise signals. In terms of stability, though, these low  $p$ -values do not inform

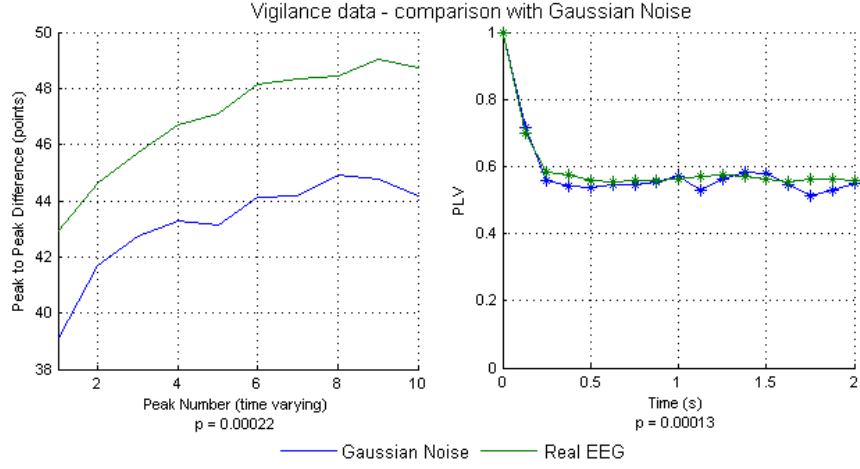


**Figure 5.9:** Peak-to-peak difference and PLV for Vigilance data. Average along segments (peak-to-peak difference: non-overlapping; PLV: overlapping). The  $p$ -values resulting of the application of the Mann Whitney U-test to the average values against Gaussian noise are listed under the plots.

	Gaussian noise	Real EEG	$p$ -value (2 sided)
Phase Difference	2.039	2.042	0.163
Standard Deviation of Phase Difference	1.310	1.307	0.215
PLV	0.561	0.578	1.346E-04
PLS	0.013	0.013	-
Synchrony Index	0.400	0.398	0.398
Average Peak-to-Peak Difference	43.753	46.264	2.221E-04

**Table 5.8:** Average results of stability tests for Vigilance data and respective  $p$ -values resulting from the application of the Mann Whitney U-test to the average values against Gaussian noise.

about which one of the signals has lower median. By inspection of the plots and the average values listed in Table 5.8, both PLV and synchrony index are too small in the case of EEG to be considered stable (as they are inferior to the noise signals).

#### 5.2.3.4 ECoG Data

In order to discard inherent noise in the EEG as a source of phase instability, the same methodology is finally applied to a set of ECoG data. The results of the phase stability analysis are presented in Figure 5.10 and Table 5.9.

Again, the analysis paradigm followed the one described in Section 5.2.2, and the PLV values were tested for significance using a surrogate test. The analysis was performed

## 5. Results

for a window of length 0.5 s and step size 0.125 s, over a five second segment. The peak-to-peak difference was calculated over the length of the segment.

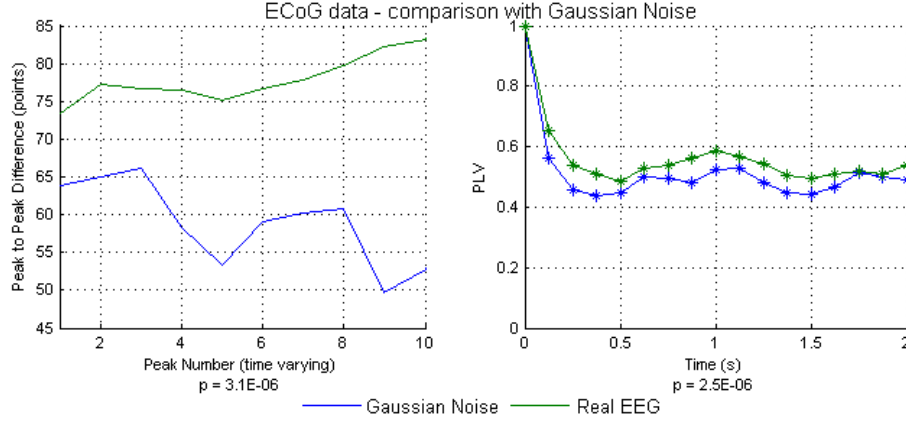


**Figure 5.10:** Peak-to-peak difference and PLV for ECoG data. Average along segments (peak-to-peak difference: non-overlapping; PLV: overlapping). The  $p$ -values resulting of the application of the Mann Whitney U-test to the average values against Gaussian noise are listed under the plots.

	Gaussian noise	Real EEG	$p$ -value
Phase Difference	1.966	2.015	0.003
Standard Deviation of Phase Difference	1.352	1.308	7.359E-05
PLV	0.504	0.549	2.506E-06
PLS	0.009	0.009	-
Synchrony Index	0.369	0.383	5.025E-05
Average Peak-to-Peak Difference	62.753	80.6050	3.071E-06

**Table 5.9:** Average results of stability tests for ECoG data and respective  $p$ -values resulting from the application of the Mann Whitney U-test to the average values against Gaussian noise.

Regarding the peak-to-peak difference, the  $p$ -value obtained from the application of the Mann Whitney U-test is significantly lower than the significance threshold ( $\alpha = 0.05$ ). This presents evidence that the ECoG does in fact not behave like Gaussian noise. By visual inspection, the EEG signal appears to have an overall less varying curve. The variation is still there, but not as erratic as the one observed for the Gaussian noise.

The main difference in this case arises when looking at the results for PLV. In fact, here it is possible to infer from the analysis, that the real EEG shows a significantly higher stability when compared to Gaussian noise. The decrease in stability is also more gradual, and remains consistently higher through the represented time in Figure 5.10.

Due to the fact that the results of the PLV for the white noise are still so high, the question of whether this apparent relatively higher phase-lock over time of the real EEG is a result of the narrow band filter, or reflects an intrinsic level of stability, remains. This result is consistent with the fact that noise and distortions are added to the EEG due to the need to acquire recordings over the skull and tissues.





# 6 Discussion and Conclusions

## 6.1 Analysis and Discussion

The present thesis had the initial purpose of studying and developing a system based on BCI for controlling the initial phase of tACS. The first part of the results goes in this direction: three algorithms are devised and tested in the sense of generating a stimulation signal from the analysis of the parameters of an original EEG signal. All three methods work as intended when applied to signals where the phase is known to be stable.

The problem arises when they are applied to real data. In this case, the results approximate those attained for random noise (Section 5.1.4). This observation raises the question of whether such a phase dependent stimulation makes sense - is the phase of the recorded EEG sufficiently stable to make sure one can apply the stimulation and guarantee that it is still in phase with the ongoing signal at that moment of stimulation?

The second part of the results deals with this question, by applying methodologies devised for quantification of phase-lock and temporal evolution of the time series. The results are discussed below.

### 6.1.1 Algorithms for Closed-Loop Stimulation

Regarding the comparison of the three methods devised in Section 5.1.3, some notes should be made, namely about the PLV results for fixed datasets. In this case, for all three methods, the measured PLV was equal. At a first glance this fact might seem odd. However, each of the methods produces a sine wave, which, despite a possible difference in the initial phase and frequency, changes in a constant manner. As this constant signal is compared to the same original signal, it is to be expected that the level of phase-lock is in fact the same. The PLV measures the amount of phase-lock, and not how good the

fit is. As such, if all the generated sine waves have similar properties, it is not surprising that the phase-lock (be it high or low) is the same.

In this same section, the Phase Adjustment Approach method was selected as the best one. Apart from the best computational time, this method is more flexible due to its simplicity, and the fact that it looks for information in the ongoing signal in a fast way. Both other methods are inferior in these terms, even if the observed outcome is very similar.

A more interesting result is seen in Subsection 5.1.4, when the selected method is applied to real data. The expected outcome would be a behaviour similar to the one obtained for the simulated EEG signal, with a possible decrease in performance, due to noisy data, artifacts, or other factors. However, the PLV and phase difference measured between the generated stimulation and the real signal show a behaviour very similar to the one obtained when comparing the stimulation signal to Gaussian noise - defined as the *worst possible outcome*. This result raises a number of questions regarding the phase of real signals. How stable is it in a determined time interval? If it is stable, then for how long? What is the available time window for a system such as the one in the present text to work as intended?

All these questions led to the more detailed study of phase stability described in Section 5.2, and discussed in the following topic.

### 6.1.2 Analysis of Phase Stability

The results presented in Section 5.2 indicate that the phase of the ongoing signal does not present enough stability to perform the type of approach suggested in Chapter 3. Indeed, upon a careful study of the evolution of the phase of a signal along time, the main conclusion is that it is completely unstable. Even in a very small time interval, the variance of the phase within one signal, seems to be erratic and unpredictable. For each of the analysed datasets, there seems to be a statistically significant evidence that the median of these phase distributions is not equal to the one observed for Gaussian-like noise time series. However, the EEG signal is even more unstable than the Gaussian noise. Thus, the main conclusion is that there is no evidence to support the hypothesis that the phase of the ongoing brain signals is stable.

This parameter was never expected to be completely stable and static along time. What was, indeed, a surprise, were the facts that: a) the phase seemed to vary faster than predicted, and b) the variation occurred in a way that resembles a random distribution.

One of the most noticeable facts in this analysis is the behaviour of Gaussian noise. As would be expected, it acquires a measurable amount of phase-lock when filtered around a small frequency band. However, despite being statistically separable from the real EEG, the overall behaviour is still very similar. This is a good indicator that the phase time series analysed for the real signals stem from signals that encompass many different frequencies over a large distribution. This means that, when band pass filtering, the influence of all these other oscillations is still present and altering the dynamics of the expected signal. What is usually assumed to exist is a phase that is not completely stable, but maintains its stability over longer periods of time.

On the other hand, the fact that it is possible to separate the two signals in a very clear way, informs that the EEG does not behave like Gaussian noise. The question as to why then the overall behaviours are similar, might be possible to answer if these time series are evaluated in different time scales. As has been shown in earlier studies, the alpha rhythm exhibits multistable states [10], and thus more information about the intrinsic behaviour of the phase over time might be achieved using multiscale methodologies, that enable the understanding of long distance correlations. This type of analysis is out of the scope of the present work.

In a study by Mazaheri et al. [51], the phase before and after the presentation of a visual stimulus was studied. For this purpose, a method very similar to the one used in this thesis was devised. In this case, it was termed *Phase Preservation Index*. The phase of a segment of a signal was compared to the phase of the same signal after a stimulus. This study aimed to help in the understanding of the origin of Event Related Potentials/Fields, and whether or not this was related to phase resetting. The study found that in the case of  $\alpha$  frequencies, the level of phase-lock remained significant for up to 0.3 s after stimulus. This was interpreted as an indicator that the pre-stimulus  $\alpha$  phase was preserved over time, even after the stimulus took place, which meant that the ongoing  $\alpha$  activity was not phase-reset by visual stimulus. The mechanism could thus be ruled out as being at the origin of ERPs/ERFs in the visual system. In the present work, however, it is shown that the stability of the ongoing spontaneous EEG is not higher than the stability reported in the referenced work.

Another interesting observation is that in the referred study the Phase-Locking Statistics was assumed to be enough to consider the presence of stability. However, for the present thesis this same statistics is applied to the Gaussian noise signals, and always returns values below the threshold for statistical acceptance of the PLV. By definition, noise is not stable, and as such the PLS would be expected to be much higher, which is not the

case. Thus, it is possible to say that the arguments used to discard phase resetting as a mechanism for the origin of ERPs are not enough.

The findings in the present thesis go in the direction of one of the main conclusions in a recent study by Cohen (July 2014) [52], where, quoting the original article, it was observed that *neural time series data violate one assumption of the analyses commonly used to analyse those data, (...) which is that the frequency structure of an oscillator does not change over time, or at least changes more slowly than the time window of analyses*. It is further shown that this *frequency sliding* is an endogenous property of neural networks. Since this frequency is *instantaneous*, it is, by definition, the first temporal derivative of the phase. Thus, according to this study, it would be expectable that the instantaneous phase of a signal also presents reduced stability.

The classical methods for analysis of EEG assume that the frequency of a neural oscillator is approximately stationary over time. This is based on the clinical definition of near sinusoidal oscillations [9]. However, the human alpha band contains multiple rhythms that apparently interact to varying degrees in different brain states [9]. However, it is in fact not surprising to think that the phase of a measured signal is not preserved, in rest conditions, over time. The measurable signals are composed of the joint activity of a huge number of neurons. When band filtered around a certain frequency of interest, the number of contributing oscillators is reduced, but still, many oscillations are contributing to the overall signal over different temporal scales. It is a growing trend to consider these dynamics in more recent research. Several studies have worked on the hypothesis that there is no real stability in the brain, but rather dynamics on different time scales [10, 53, 54]. The results attained in the present thesis are thus consistent with the more recent work on EEG rhythms.

## 6.2 General Conclusions and Future Directions

The present thesis started with a very well defined goal of making the first steps towards a closed system that detects the phase and frequency of an ongoing signal, and adjusts a stimulation signal to be delivered by tACS. The first part of the project concerns itself with the problem of defining algorithms that fulfil this purpose. Despite these needing some finer adjustments, the problem encountered when applying the best of the three methods to real data, forced the direction of the thesis into a different topic: the stability of the spontaneous EEG phase over short intervals of time.

As a general conclusion, the first thing to note, is that the initial phase adjustment approach suggested in Sections 4.2 and 5.1 will not fulfil their purpose, as the phase changes too fast.

Addressing the phase problem, this should be separate from the first main goal of the thesis. More insight is necessary, as the current literature is diffuse and at times contradictory when it comes to the topic of phase. The fact that it is seen as a well studied and rather simple problem, has resulted in a continuous dismissal of the real properties of phase. As was referred above, the fact that it changes too fast, in an unpredictable way, was not expected, even upon conversations with experts in brain stimulation. This indicates that there is a wrong paradigm in classical EEG analysis. Very recently, this problem was pointed out, [52], but although some other studies also go in this direction, the problem still persists in the area. This paradigm is that the frequencies (and inherently, the stability of phase) of a signal, present changes that are slow enough to be dismissed upon analysis.

The problem regarding the onset of stimulation might be possible to overcome, even before understanding these dynamics in a deeper way, if a different type of approach is attempted. At this point, there are several possibilities to consider. The first is that if the artifact problem referred to in Section 3.3.1 was overcome, a variation of the proposed algorithms could be attempted. On the other hand, the intervals considered for the generation of the stimulation signals were rather long. As was discussed above, the real EEG presents very variable dynamics, and thus, much smaller windows should be considered. Perhaps a possibility could be to use very small windows, on signals with very high resolution (i.e., high sampling frequency). This should enable a much finer study of the phase and frequencies of a signal. Another point is that the current methods dealt with frequency as a constant parameter over time. However, this assumption will have an influence in the phase problem too, and thus new solutions should be searched for. All three methods are quite straightforward, and, although often simple is better, in this case it might be beneficial to use more advanced techniques, and a more complex approach to the problem, perhaps even considering non-linear methodologies. Since the time factor becomes extremely important, a possibility for further improvement might be to let the algorithms run on dedicated, embedded processing devices. This is out of the scope of the present thesis, though, and would require a more multidisciplinary team to accomplish.

This thesis represents a first important step into understanding crucial problems in the concept of tACS-BCI loops, and points out problems that need further investigation.

The three different algorithms that were developed work well on stable data, but fail when applied to real EEG signals. Upon further analysis, it is possible to infer that the phase of a real EEG signal is not more stable than that of Gaussian noise. Thus, this work disproves the classical EEG analysis, and supports recent research on the claim that the variability of frequency and phase over time cannot be dismissed.

# Bibliography

- [1] Herrmann, C.S., et al., *Transcranial alternating current stimulation: a review of the underlying mechanisms and modulation of cognitive processes.*, Front Hum Neurosci, 7: 279, 2013, doi:10.3389/fnhum.2013.00279. 1, 9, 10
- [2] Zaehle, T., Rach, S., Herrmann, C.S., *Transcranial alternating current stimulation enhances individual alpha activity in human EEG.*, PLoS ONE, 5(11): 13766, 2010, doi:10.1371/journal.pone.0013766. 1, 10
- [3] Gundlach, C., *Modulation of somatosensory oscillations by means of transcranial alternating current stimulation*, 2010. 1, 10
- [4] Busch, N.A., Dubois, J., VanRullen, R., *The phase of ongoing EEG oscillations predicts visual perception.*, J. Neurosci., 29(24): 7869–76, 2009, doi:10.1523/JNEUROSCI.0113-09.2009. 1, 7, 8
- [5] Varela, F.J., et al., *Perceptual framing and cortical alpha rhythm*, Neuropsychologia, 19(5): 675–686, 1981, doi:doi:10.1016/0028-3932(81)90005-1. 1, 7
- [6] Saladin, K.S., *Anatomy & Physiology - The Unity of Form and Function 3rd Edition*, The McGraw-Hill Companies, 2003. 5, 6
- [7] Blinowska, K., Durka, P., *Wiley Encyclopedia of Biomedical Engineering*, chap. Electroencephalography (EEG), John Wiley & Sons, Inc., Hoboken, New Jersey, 2006. 6, 7, 14
- [8] Klimesch, W., Sauseng, P., Hanslmayr, S., *EEG alpha oscillations: the inhibition-timing hypothesis.*, Brain Res Rev, 53(1): 63–88, 2007, doi:10.1016/j.brainresrev.2006.06.003. 7
- [9] Nunez, P.L., Wingeier, B.M., Silberstein, R.B., *Spatial-temporal structures of human alpha rhythms: Theory, microcurrent sources, multiscale measurements, and global binding of local networks*, Human Brain Mapping, 13(3): 125–164, 2001, doi:10.1002/hbm.1030, URL <http://dx.doi.org/10.1002/hbm.1030>. 7, 34, 64
- [10] Freyer, F., et al., *A canonical model of multistability and scale-invariance in biological systems.*, PLoS Comput. Biol., 8(8): e1002634, 2012, doi:10.1371/journal.pcbi.1002634. 7, 63, 64

- [11] Burkitt, G.R., et al., *Steady-state visual evoked potentials and travelling waves*, Clinical Neurophysiology, 111(2): 246–258, 2000, doi:[http://dx.doi.org/10.1016/S1388-2457\(99\)00194-7](http://dx.doi.org/10.1016/S1388-2457(99)00194-7), URL <http://www.sciencedirect.com/science/article/pii/S1388245799001947>. 7
- [12] Polanía, R., et al., *The importance of timing in segregated theta phase-coupling for cognitive performance.*, Curr. Biol., 22(14): 1314–8, 2012, doi:10.1016/j.cub.2012.05.021. 8
- [13] Reato, D., et al., *Low-intensity electrical stimulation affects network dynamics by modulating population rate and spike timing.*, J. Neurosci., 30(45): 15 067–79, 2010, doi:10.1523/JNEUROSCI.2059-10.2010. 8, 9, 10
- [14] Pascual-Leone, A., et al., *The plastic human brain cortex.*, Annu. Rev. Neurosci., 28(28): 377–401, 2005, doi:10.1146/annurev.neuro.27.070203.144216. 8
- [15] Terney, D., et al., *Increasing human brain excitability by transcranial high-frequency random noise stimulation.*, J. Neurosci., 28(52): 14 147–55, 2008, doi:10.1523/JNEUROSCI.4248-08.2008. 8, 9
- [16] Antal, A., Paulus, W., *Transcranial alternating current stimulation (tACS).*, Front Hum Neurosci, 7: 317, 2013, doi:10.3389/fnhum.2013.00317. 8, 9
- [17] Rossi, S., et al., *Safety, ethical considerations, and application guidelines for the use of transcranial magnetic stimulation in clinical practice and research.*, Clin Neurophysiol, 120(12): 2008–39, 2009, doi:10.1016/j.clinph.2009.08.016. 8
- [18] Reato, D., et al., *Effects of weak transcranial alternating current stimulation on brain activity-a review of known mechanisms from animal studies.*, Front Hum Neurosci, 7: 687, 2013, doi:10.3389/fnhum.2013.00687. 9, 11
- [19] Pogosyan, A., et al., *Boosting cortical activity at Beta-band frequencies slows movement in humans.*, Curr. Biol., 19(19): 1637–41, 2009, doi:10.1016/j.cub.2009.07.074. 9
- [20] Antal, A., et al., *Comparatively weak after-effects of transcranial alternating current stimulation (tACS) on cortical excitability in humans.*, Brain Stimul, 1(2): 97–105, 2008, doi:10.1016/j.brs.2007.10.001. 9
- [21] Graimann, B., Pfurtscheller, G., Allison, B., *Brain-Computer Interfaces - Revolutionizing Human-Computer Interaction*, The Frontiers Collection, Springer, n/a 2010, doi:10.1007/978-3-642-02091-9. 11, 12, 17
- [22] Dornhege, G.t.a., *Toward brain-computer interfacing*, Neural Information Processing Series, The MIT Press, Cambridge, Massachusetts, 2007. 11, 12
- [23] Wolpaw, J.R., Birnbauer, N.e.a., *Brain-computer interface technology: a review of the first international meeting - Rehabilitation Engineering*, IEEE Transactions on, IEEE Transactions on Rehabilitation Engineering, 8(2): 164–173, 2000. 11



- 
- [24] Vallabhaneni, A., Wang, T., He, B., *Neural Engineering*, chap. Brain-Computer Interface, 85–121, Springer US, 2005, doi:10.1007/b112182. 11
  - [25] Birnbauer, N., *Slow Cortical Potentials: Plasticity, Operant Control, and Behavioral Effects*, Neuroscience Update, 5(74): 74–78, 1999, doi:10.1177/107385849900500211. 11
  - [26] Schalk, G., et al., *BCI2000: a general-purpose brain-computer interface (BCI) system.*, IEEE Trans Biomed Eng, 51(6): 1034–43, 2004, doi:10.1109/TBME.2004.827072. 13
  - [27] Spüler, M., Rosenstiel, W., Bogdan, M., *Principal component based covariate shift adaption to reduce non-stationarity in a MEG-based brain-computer interface*, EURASIP Journal on Advances in Signal Processing, 2012(1):129, 2012, doi:10.1186/1687-6180-2012-129, URL <http://dx.doi.org/10.1186/1687-6180-2012-129>. 14
  - [28] Cross, M., *Chapter 6: Power Spectrum*. 14
  - [29] Semmlow, J.L., *Biosignal and Biomedical Image Processing: MATLAB-Based Applications*, Signal Processing and Communications, Marcel Dekker, Inc., 2004. 15, 16, 18
  - [30] Le Van Quyen, M., et al., *Comparison of Hilbert transform and wavelet methods for the analysis of neuronal synchrony*, Journal Of Neuroscience Methods, 111: 83–98, 2001, doi:10.1016/S0165-0270(01)00372-7. 18, 20, 21, 22
  - [31] Kschischang, F.R., *The Hilbert Transform*, October 2006, the Edward S. Rogers Sr. Department of Electrical and Computer Engineering University of Toronto. 18
  - [32] Picinbono, B.C., *On instantaneous amplitude and phase of signals*, IEEE Transactions on Signal Processing, 45(3): 552–560, 1997, URL <http://dblp.org/db/journals/tsp/tsp45.html#Picinbono97>. 18, 20
  - [33] Lab, C., *The Hilbert Transform*, Web Content, 2007, <http://www.cjs-labs.com/sitebuildercontent/sitebuilderfiles/hilberttransform.pdf>. 19
  - [34] Lachaux, J.P., et al., *Measuring phase synchrony in brain signals*, Human Brain Mapping, 8: 194–208, 1999, doi:10.1002/(SICI)1097-0193(1999)8:4<194::AID-HBM4>3.0.CO;2-C. 20, 21, 23
  - [35] Carter, G.C., *Coherence and time delay estimation*, Proceedings of the IEEE, 75(2): 236–255, Feb 1987, doi:10.1109/PROC.1987.13723. 20
  - [36] Lachaux, J.P., et al., *Estimating the time-course of coherence between single-trial brain signals: an introduction to wavelet coherence*, Neurophysiologie Clinique/Clinical Neurophysiology, 32(3): 157–174, 2002, doi:http://dx.doi.org/10.1016/S0987-7053(02)00301-5. 21
  - [37] Aydore, S., Pantazis, D., Leahy, R.M., *A note on the phase locking value and its properties.*, Neuroimage, 74: 231–44, 2013, doi:10.1016/j.neuroimage.2013.02.008. 21
  - [38] Shannon, C.E., *A mathematical theory of communication*, Bell System Technical Journal, The, 27(3): 379–423, July 1948, doi:10.1002/j.1538-7305.1948.tb01338.x. 22

- [39] Walter, A., et al., *Coupling BCI and cortical stimulation for brain-state-dependent stimulation: methods for spectral estimation in the presence of stimulation after-effects.*, in *Frontiers in Neural Circuits*, vol. 6, 87, doi: 10.3389/fncir.2012.00087, 10 2012, doi: 10.3389/fncir.2012.00087. 25, 26, 28, 40
- [40] Walter, A., et al., *Dynamics of a Stimulation-evoked ECoG Potential During Stroke Rehabilitation - A Case Study*, in *NEUROTECHNIX 2013 - International Congress on Neurotechnology, Electronics and Informatics*, 241–243, 09 2013. 25, 26
- [41] Chen, L.L., et al., *Real-time brain oscillation detection and phase-locked stimulation using autoregressive spectral estimation and time-series forward prediction.*, *IEEE Trans Biomed Eng*, 60(3): 753–62, 2013, doi:10.1109/TBME.2011.2109715. 26
- [42] Boyle, M.R., Frohlich, F., *EEG feedback-controlled transcranial alternating current stimulation*, in *Neural Engineering (NER), 2013 6th International IEEE/EMBS Conference on*, 140–143, Nov 2013, doi:10.1109/NER.2013.6695891. 26
- [43] Helfrich, R.F., et al., *Entrainment of brain oscillations by transcranial alternating current stimulation.*, *Curr. Biol.*, 24(3): 333–9, 2014, doi:10.1016/j.cub.2013.12.041. 27
- [44] g.tec medical engineering GmbH, *gtecProductCatalogue 2013/2014*, Tech. rep., <http://www.gtec.at/Products/Hardware-and-Accessories/g.USBamp-Specs-Features>, 2013. 29
- [45] neuroConn GmbH, *NeuroConn DC Stimulator Plus: Measuring and Modulating Brain Activity*, Product Brochure, 06 2012. 29
- [46] Burg, J.P., *Modern spectrum analysis*, chap. A new analysis technique for time series data, IEEE Press : sole worldwide distributor (exclusive of IEEE), Wiley, 1968, URL <http://books.google.pt/books?id=bZFRAAAAMAAJ>. 38
- [47] Burg, J.P., *Maximum Entropy Spectral Analysis*, in *Proceedings of the 37th Meeting of the Society of Exploration Geophysicists*, Oklahoma City, Oklahoma, 1967. 38
- [48] Spüler, M., Rosenstiel, W., Bogdan, M., *Online adaptation of a c-VEP Brain-computer Interface(BCI) based on error-related potentials and unsupervised learning.*, *PLoS ONE*, 7(12): –51 077, 2012, doi:10.1371/journal.pone.0051077. 40
- [49] Spüler, M., et al., *Online use of error-related potentials in healthy users and people with severe motor impairment increases performance of a P300-BCI.*, *Clin Neurophysiol*, 123(7): 1328–37, 2012, doi:10.1016/j.clinph.2011.11.082. 40
- [50] Sauseng, P., et al., *Are event-related potential components generated by phase resetting of brain oscillations? A critical discussion.*, *Neuroscience*, 146(4): 1435–44, 2007, doi: 10.1016/j.neuroscience.2007.03.014. 53
- [51] Mazaheri, A., Jensen, O., *Posterior alpha activity is not phase-reset by visual stimuli.*, *Proc. Natl. Acad. Sci. U.S.A.*, 103(8): 2948–52, 2006, doi:10.1073/pnas.0505785103. 63

- [52] Cohen, M.X., *Fluctuations in oscillation frequency control spike timing and coordinate neural networks.*, J. Neurosci., 34(27): 8988–98, 2014, doi:10.1523/JNEUROSCI.0261-14.2014. 64, 65
- [53] Jensen, O., Mazaheri, A., *Shaping functional architecture by oscillatory alpha activity: gating by inhibition.*, Front Hum Neurosci, 4: 186, 2010, doi:10.3389/fnhum.2010.00186. 64
- [54] Omata, K., et al., *Spontaneous Slow Fluctuation of EEG Alpha Rhythm Reflects Activity in Deep-Brain Structures: A Simultaneous EEG-fMRI Study.*, PLoS ONE, 8(6): e66869, 2013, doi:10.1371/journal.pone.0066869. 64